ADSORPTION OF Cu (II) AND Cd (II) BY CHITINOUS POLYMERS

By

Hong Zhang

RECOMMENDED:

Advisory Committee Chair

Chair, Department of Civil and Environmental Engineering

APPROVED:

Dean, College of Engineering and Mines

Dean of the Graduate School

December 11, 2006

Date

ADSORPTION OF Cu (II) AND Cd (II) BY CHITINOUS POLYMERS

A

THESIS

Presented to the Faculty

of the University of Alaska Fairbanks

in Partial Fulfillment of the Requirements

for the Degree of

MASTER OF SCIENCE

By

Hong Zhang, M.S, B.S

Fairbanks, Alaska

December 2006

Abstract

Heavy metal contamination has emerged as a major health problem worldwide. Biosorption, using biological waste products as sorbents, may provide a cost effective treatment strategy. The current study investigated several types of biomass, generated from waste crab shells, as bio-sorbents to remove cadmium and copper in a batch reaction system. Isotherm studies suggested that uptake increased with increasing number of amine groups, i.e. increasing degree of deacetylation (DDA) as measured by hydrogen nuclear magnetic resonance (^{1}H-NMR) as well as Fourier Transform Infra-red (FTIR) spectroscopy. Potentiometric titration was shown not to be a valid method in measuring the DDA for medium DDA range. pH was proven to be a main factor affecting the adsorption because of the considerable competition of protons for the binding sites at low pH. Cu^{2+} had higher affinity than Cd^{2+} to the chitinous polymer. Metal adsorption was elevated by high ionic strength because of more adsorption sites becoming accessible as a result of significant expansion of the network under high ionic strength. Sulfate as salt, added in the solution, greatly stimulated the adsorption of metal ions by reducing the repulsion force between the charged surface and the metal cations.

Table of Contents

List of Figures

List of tables

List of Symbols

B_r	Remaining full width at half of maximum (FWHM)
B_o	Observed width
B_i	Instrumental effect
C	Concentration of NaOH
C_0,	Initial metal concentration
C_{eq},	Equilibrium metal concentration
CrI	Crystallinity index
I_{020}	Maximum crystallinity diffraction pattern intensity
I_{am}	Amorphous diffraction pattern intensity at $2\theta \approx 16^{o}$
K_T	Boltzman's constant
L	Average crystallite size
M	Sorbent mass
pK_a	Dissociation constant
pK_0	Intrinsic dissociation constant
q	Uptake amount of metal per gram of sorbent (mg/g)
Q_m	Maximum swelling ratio
S*	Ionic strength
v_1	NaOH volume consumed at the first inflexion point (mL)
v_2	NaOH volume consumed at the second inflexion point (mL)

ν_e	Effective number of chains in the network
V	Volume of the solution containing sorbent
V_1	Molar volume of solvent
V_0	Volume of unswollen network
V_u	Molecular volume of the repeating unit
W	Sample weight (g)
α	Degree of dissociation
ε	Electron charge
λ	Wavelength of the X-ray
θ	Bragg angle
i	Number of electronic charges per polymer unit
χ_1	Parameter expressing the first neighbor interaction free energy
$\Delta\Psi$	Electrostatic potential difference

Acknowledgments

I want to thank many people for their kind help in preparing this thesis. First of all, I would like to thank my advisor: Dr. Silke Schiewer, who provided me this great opportunity to pursue a degree at UAF. I really enjoyed diving into diverse chemistry subjects and doing independent research here. I am also grateful to my advisory committee members: Dr. Daniel White, Dr. Dave Barnes and Dr. Thomas Trainor for their valuable advice on my research. I especially would like to thank Dr. Trainor for teaching me the molecular scale knowledge related to adsorption.

The contribution of Dr. Tom Green deserves a special mention; he did not just teach me the basics of the NMR technique, but also helped out with my sample analysis and data interpretation. Special thanks also to Dr. Mike Whalen, who provided me the opportunity to learn to use the x-ray powder diffraction device.

I also would like to express my gratitude to all the staff working in the Water and Environmental Research Center (WERC) Laboratory, especially Shane Billing, who helped me a lot in metal analysis and TOC analysis. An extra thanks to Sarah Seelen, who always made it possible for me to use the wiggle bugs. Finally, I would like to thank my family and friends, for their support all through my life. Thank you all.

Chapter 1

Introduction

1.1 Biosorption and biosorbents

Heavy metal ions dissolved in aqueous solution can be highly toxic to humans and aquatic life, even in very low concentrations. For example, the maximum contaminant level (MCL) for Cu^{2+} is 1.3 ppm, Pb^{2+} is 0.015 ppm and Cd^{2+} is 0.005 ppm (US EPA, 2006). Removal of heavy metal ions from water is essential. Various approaches have been developed to achieve this goal. Physical-chemical methods such as chemical precipitation, chemical oxidation or reduction, filtration, ion exchange, reverse osmosis and membrane technologies are widely used (Davis et al., 2003). However, these conventional processes may be ineffective or expensive, especially when the heavy metal concentration is below 100 mg/L. It is critical to search for both efficient and cost effective methods to remove the heavy metals in the low concentration range.

Biosorption might provide an answer (Volesky, 1990). Biosorption is a process that utilizes inexpensive non-living biomass to sequester toxic heavy metal ions and is particularly suited for the low concentration range. The mechanism of biosorption includes one or more of passive accumulation processes such as ion exchange, surface complexation, adsorption and micro-precipitation. This process combines the advantages of being highly efficient at metal removal and much more cost effective than comparable techniques such as ion exchange, because low cost biomass is used as sorbents. Materials that have been investigated include biomass abundant in nature such as seaweed and tree leaves or waste products from industry such as citrus peels, waste yeast and crab shells.

The purpose of this study is to investigate the adsorption of copper and cadmium on chitinous polymers extracted from crab shells, which include research on the physical-chemical properties of the sorbent, the adsorption isotherms and the influence of factors such as the pH and ionic strength.

The fisheries industry produces large quantities of crab shells as waste products each year all around the world. Crab shells consist of three main components: $CaCO_3$, protein and chitin (poly-N-acetyl-D-glucosamine), which makes up 10-40% by weight (Rhazi et al., 2000). Chitin can be extracted from crab shells through decalcification with acid and deproteination with a diluted base bath. Chitosan (poly-D-glucosamine) can be obtained by deacetylation of chitin with concentrated alkali treatment at high temperature (Muzzarelli, 1977).

Crab shell, along with its derivatives: acid-washed crab shell, chitin and chitosan were reported as major sinks for heavy metals such as copper, zinc, mercury and cadmium (Jha et al., 1998; Kurita et al., 1979). Kim et al. (2001) indicate that crab shell was more capable of adsorbing Pb^{2+} than both chitin and chitosan, and the uptake on chitin and chitosan was almost the same. Micro-precipitation of $PbCO_3(s)$ and $Pb_3(CO_3)_2(OH)_2(s)$ was suggested to be the main mechanism in that case. Niu (2003) reported that the acid-washed crab shells adsorbed metal oxyanions. Suder and Wightman (1983) observed that Zn^{2+} and Cd^{2+} adsorbed to both chitin and chitosan, with chitosan performing as a better sorbent. Similar results were achieved by Kurita et al. (1977), who suggested the amount of accessible amino groups determined the amount of metal uptake

by the polymer. Using the cheap crab shell based sorbents to remove metal ions could benefit the world's seafood industry and protect the aquatic environment.

1.2 Properties of chitin and chitosan

Although the raw crab shell and acid washed crab shell were sometimes used as the sorbent, it was the chitin and chitosan that attracted the most attention.

1.2.1 Characteristics of chitin

Chitin is a natural polysaccharide abundant in many sources like fungi, or the exoskeleton of insects and crustaceans such as prawns and crabs. It is a polysaccharide based on units of acetylglucosamine (more precisely N-acetyl-D-glucos-2-amine). These are linked together in β-1,4 fashion (in a similar manner to the glucose units which form cellulose). The molecular formula of chitin $(C_8H_{13}NO_5)_n$ and its chemical structure are shown in Fig.1.1.

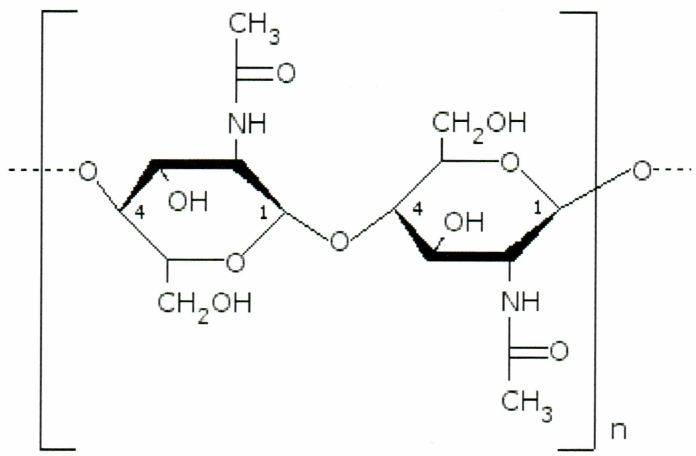

Fig. 1.1 Molecular structure of chitin

In effect, chitin may be described as cellulose with one hydroxyl group on each monomer replaced by an acetyl-amine group. This allows for increased hydrogen

bonding between adjacent chitin chains, giving the polymer increased strength and preventing it from dissolving in water and diluted acids. Although it does not dissolve in normal circumstances, chitin is ready to swell in water, acid and base. (Muzzarelli, 1977).

In living systems, chitin molecular chains are held together by the hydrogen bonding between the chains, forming crystallite structures called chitin micro-fibers with diameters around 2.8 nm, and those microfibers are embedded in a six stranded protein helix (Muzzarelli, 1977). After the protein is removed by a hot base wash, chitin remains as the product. Chitin itself is seldom used as a sorbent, but rather serves as an intermediary to produce its derivative chitosan. According to some researchers (Guibal et al., 1999), chitosan is a preferred sorbent compared to chitin because the amino groups provide better binding sites than chitin amide groups.

1.2.2 Production of chitosan

Chitosan (poly-D-glucosamine) with its chemical structure shown in Fig. 1.2 can be obtained by removing the acetyl group from some chitin units. Normally, the acetyl groups on the chitin are not totally removed, and the mole fraction of the glucosamine residue (GlcN, a unit of chitosan) in the polymer chain is defined as the degree of deacetylation (DDA) (Baxter et al., 1992). Despite the specific chemical designation, the names "chitin" or "chitosan" each cover a range of polymers having different acetyl content. According to Khor (2001), chitinous polymers with a degree of deacetylation (DDA) < 50% are commonly called chitin and the term chitosan is reserved to those having DDA >50%.

There are two common methods to conduct the deacetylation via homogeneous and heterogeneous reactions. In homogeneous deacetylation, chitin is dissolved in sodium hydroxide solution by stirring vigorously with crushed ice below 0°C to obtain alkali chitin (Sannan et al., 1975). Deacetylation happens homogeneously in the solution when the solution is warmed up to room temperature and above. The desired DDA was achieved by controlling the temperature and reaction time with high temperature and long reaction time resulting in higher DDA. In heterogeneous deacetylation, chitin is dispersed in concentrated sodium hydroxide solution at elevated temperature. The reaction starts from the interface between chitin and the solution and the extent of deacetylation increases with the base concentration, reaction time and reaction temperature (Kurita et al., 1977).

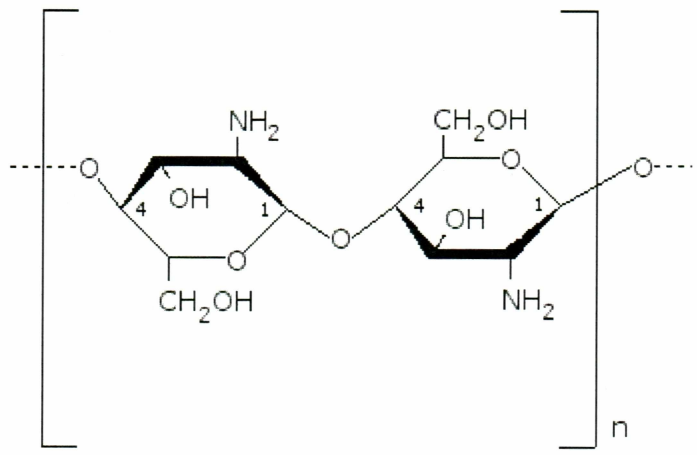

Fig. 1.2 Molecular structure of chitosan

1.2.3 Charge distribution on chitosan

The amino group on chitosan can be positively charged through the reaction described in equation 1-1 and cause the polymer to dissolve in most diluted organic acids

and mineral acids like HCl, HBr, HNO_3 and $HClO_4$. Chitosan is insoluble in diluted H_2SO_4. The dissociation constant of the conjugated acid is obtained from the equilibrium:

$$R\text{-}NH_3^+ \longrightarrow R\text{-}NH_2 + H^+ \quad (1\text{-}1)$$

$$K_a = \frac{[R-NH_2][H^+]}{[R-NH_3^+]} \quad (1\text{-}2)$$

In fact the apparent dissociation constant of chitosan is not a constant but depends on the degree of dissociation at which it is determined. The pK_a can be calculated using Katchalsky's equation (Sorlier et al., 2001):

$$pK_a = pH + \log((1-\alpha)/\alpha) = pK_0 - \varepsilon\,\Delta\Psi(a)/k_T \quad (1\text{-}3)$$

Where $\Delta\Psi$ is the difference in electrostatic potential between the surface of the poly-ion and the reference α is the degree of dissociation, k_T is the Boltzman's constant and ε is the electron charge. Extrapolation of the pK_a value to α=1, where the polymer becomes uncharged and hence the electrostatic potential becomes zero, enables estimating the value of the intrinsic dissociation constant of the ionizable groups, pK_0. The value obtained, ~6.5, is independent of the degree of N-acetylation, whereas the pK_a value is highly dependent on this factor. The apparent pK_a values of the amino group vary in the range from 6.2 to 7.3 as a function of DDA and degree of dissociation.

The protonation significantly affects the adsorption of metal cations as well as oxyanions. The charged amino groups favor the adsorption of anions, such as chromate and arsenate because of the electrostatic attraction (Niu et al., 2003; Kim et al. 1997), but

weaken the adsorption of metal cations, especially those that don't strongly react with the amino group, through the competition by protons (Piron and Domard, 1998).

1.2.4 Crystallinity and molecular weight of chitosan

In fact, during the process of deacetylation, not only are the side groups on the chain structure changed, but the conformation of the polymer is affected also. As stated before, chitin has a crystallite structure because of the hydrogen bonding between chains. After removing some of the acetyl groups, the crystallite structure is partly destroyed. The chitosan configuration was characterized as partly crystalline having chains organized into ordered ranges called crystallites dispersed in an otherwise amorphous matrix (Jaworska et al., 2003). It is believed that the intra- and intermolecular hydrogen bonds in the crystalline regions are responsible for the resistance of chitin/chitosan to swell or dissolve in water or diluted acid (Guo et al., 2002). The deacetylation under homogeneous conditions seems to take place randomly along the chain producing a random type copolymer, resulting in a rapid decrease in crystallinity and better solubility of the product. The heterogeneous deacetylation is likely to produce block distribution chitosan. It was noted that the homogeneous chitosan was almost amorphous for DDA above 40%, while heterogeneous samples up to DDA 80% maintained some crystallinity (Kurita et al., 1977). To avoid significant dissolution of the sorbent, the crystallite structure has to be maintained when producing of chitosan, thus heterogeneous deacetylation was chosen for this study.

Another factor, which is also changed during deacetylation, is the molecular weight (MW) (Mao et al., 2004), with the MW of chitin usually more than million

Daltons. During the deacetylation, high temperature, high concentration of base, dissolved oxygen, and sheer stress cause degradation of the polymer. Treatment with 40% NaOH solution at 100° C reduced the MW to 80k Dalton in 2 hours. The MW decreased to 50k Dalton, if 50% NaOH solution was used at the same temperature and time. If the reaction temperature was 120° C, the MW reduced to 40k Dalton in 40% NaOH and to 20k Dalton in 50% NaOH solution in 2 hours (Kristbergsson et al., 2003).

Together with DDA and crystallinity, the molecular weight (MW) controls the solubility of chitosan samples. Low molecular weight samples (MW < 50k Dalton) dissolve easily in a neutral to slightly basic environment (pH 7-8), while a pH below 6.5 is required for samples with MW > 400kD. In the current study, the deacetylation environment was chosen so that the sorbent remains relatively stable in neutral and mildly acidic conditions.

1.2.5 Crosslinking of chitosan

Due to the instability of chitosan in acidic solutions (Filar et al., 1977), chemical crosslinking has often been used to enhance the acidic resistance of the material. The crosslink can be covalent or ionic. For covalent crosslinking, chitosan is dissolved in an acidic aqueous medium, and then the reactant, for example dialdehydes, diethyl squarate, oxalic acid or genipin, is added in the solution as a crosslinker to precipitate chitosan (Berger et al., 2001). In case of ionic crosslinking, metallic anions, such as Mo(VI) or Pt(II), as well as anionic molecules, such as phosphate and polyphosphates (Berthold et al., 1996) are commonly used as crosslinkers. Simply soaking the polymer in the electrolyte partly crosslinks the polymer, depending on the expansion of the network. The

stability can be greatly improved after crosslinking; however, since most of the crosslinking agent acts on the amine groups instead of the hydroxyl groups in chitosan, some of the amine groups, which are generally known to be the main adsorption sites for heavy metal ions, will be consumed in the crosslinking reaction. Therefore, the adsorption capacity for metal ions can be reduced (Li and Bai, 2005). However, since the crosslinking prevents the sorbent from dissolving in acid, the uptake of oxyanions, which is more efficient in an acidic environment such as pH 3, can be improved by crosslinking. For example, it was reported by Muzzarelli, (1977) that conditioning chitosan with H_2SO_4 increased the sorbent's uptake capacity for vanadate, chromate and molybdate. A similar result was observed by Lasko et al. (2004) during a study of sulfuric acid pretreatment to improve the adsorption of Cr(VI) by chitosan.

1.3 Mechanisms for metal adsorption by chitin and chitosan

Intensive research has been done to determine the mechanisms of metal adsorption by chitin and chitosan. Suder and Wightman (1983) studied the uptake of Cd^{2+} and Zn^{2+} by chitin and chitosan in solution and indicated that simple ion adsorption on the surface of the sorbent was not the dominant uptake mechanism. Nodule formation on the polymer surface was observed though SEM. Piron and Domard (1997) demonstrated that chitosan formed stable uncharged complexes with uranyl ions at pH 6.5-7.5. They suggested that ionic strength does not affect the adsorption, which is indicative of chemisorption. Park et al. (1984) reported that only Cu^{2+}coordinated with chitosan showed an adsorption band at 265nm in a UV spectrum, while addition of other divalent cations, such as Mg^{2+}, Ca^{2+}, Zn^{2+} and Cd^{2+} on chitosan did not result in a noticeable

spectral change above 240nm when the pH was below 5.8. This did not mean that other cations could not coordinate with chitosan. However, at low pH values, only copper competed strong enough with protons for the active sites. The evidence of Zn^{2+} and Cd^{2+} complexation was provided by x-ray photoelectron spectroscopy (XPS) experiments. The XPS bonding energy for the chitosan nitrogen before adsorption was N1s=398.8 ev, while after adsorption of cadmium, N1s + Cd^{2+} =399.1 ev and after adsorption of zinc N1s + Zn^{2+}=399.6 ev (Suder and Wightman, 1983). The chemical shift observed by XPS indicated the formation of Zn^{2+}-chitosan and Cd^{2+}-chitosan complexes.

Chitosan is believed to be a better sorbent for metal cations compared to chitin because of its significant amount of free amino groups. It was suggested that during the adsorption of divalent metals such as Cd^{2+} (Wang et al., 2001) and Zn^{2+} (Ding et al., 2003), the empty 4s/5s and 4p/5p orbital of the metal ions mixed to form 4 sp3 hybrid orbitals that can accommodate the lone pair electrons from NH_2. According to this mechanism, the free amino group is more active for metal binding than the acetyl-amine group (also called amide group). Because of the resonance of the double bond (Fig.1.3), the amide group does not truly have lone pair electrons to supply to the empty orbital of metal cations. Therefore, determination of DDA is necessary to estimate the amount of active sites and predict the adsorption capacity of chitosan.

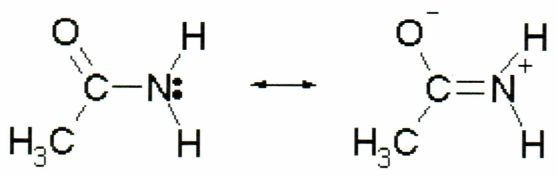

Fig. 1.3 Resonance of amide

Chapter 2

Hypotheses and objectives

Although the usage of chitin and chitosan to treat heavy metal contaminants has been widely studied in the last 20 years, as reviewed in the previous chapter, several questions still remain unanswered, which inspired the hypotheses of this research. In this chapter, each hypothesis is proposed and followed by a testing approach. Accomplishing each test will lead us closer to the main objective of this research: to understand more about the interaction between the metal ions and the chitinous polymers and predict adsorption results.

2.1 Reliability of DDA measurement methods

Deacetylation of chitin results in one of its most important derivatives: chitosan. The degree of deacetylation (DDA) represents the amount of free amino groups on the polymer and is also related to many intrinsic properties of the sorbent, such as molecular weight and crystallinity. To characterize the sorbent, the DDA must be addressed.

Measurement of DDA was frequently conducted though potentiometric titration (Rhazi et al., 2000; Guo et al., 2002; Mima et al., 1983) along with hydrogen nuclear magnetic resonance (^{1}H-NMR) as well as Fourier Transform Infra-red (FTIR) spectroscopy. The NMR method was proven to be reliable and is used in the pharmaceutical industry as a standard method for DDA measurement (Lavertu et al., 2003). However, the method is relatively expensive and the facility is not widely available. The FTIR method and potentiometric titration are cheaper and easier ways to detect the DDA, but their reliability is questioned.

Hypothesis 1): FTIR is a valid method to measure the DDA, only when the correct baseline method is chosen and calibration is conducted.

Test: Deacetylation of chitin was conducted at different temperatures for different length of time, which resulted in several batches of chitosan samples with different DDA. The NMR DDA were first acquired as a standard, and the DDA obtained through the FTIR method were evaluated by comparing with the standard.

In the case of potentiometric titration, the problem arises from the lack of quantification of the permeation and dissolution of the material. Chitosan becomes increasingly permeable and soluble when the DDA increases (Chen and Hua, 1996). However, since not all the samples with different DDA are soluble, the question arises whether all the deacetylated parts dissolve or are exposed for titration. In other words, does the amount of titrable sites equal the total amount of amino groups?

Hypothesis 2): Potentiometric titration is not a valid method to measure the DDA.

Test: Samples with different DDA were characterized by potentiometric titration. Data gained were compared with data from NMR to determine if the number of titrable sites was equal to the number of amine groups according to NMR.

2.2 Selection of the best sorbent

As stated in the introduction, crab shells consist of three main elements: $CaCO_3$, protein and chitin. Stepwise acid and base wash will remove the $CaCO_3$ and protein and chitin will remain, from which chitosan can be made. Thus, the question is which one is the best sorbent: raw crab shell, acid-washed crab shell, chitin or chitosan? How is DDA of the chitinous polymer related to the adsorption capacity?

Hypothesis 3): For most of the metal ions, chitosan is a superior ligand because of the great amount of amino groups on the sorbent. The adsorption capacity of chitosan increases with the increase of DDA. Chitin adsorbs a small amount of metal while the raw crab shell should not show significant uptake. The acid washed crab shell had chitin embedded in protein, which should show different behavior than both chitin and chitosan because the uptake of metal, if any, is accomplished by protein instead of chitin.

Test: Copper and cadmium were chosen as the target metals and four types of sorbents: raw crab shell, acid-washed crab shell, chitin and chitosan were tested for their adsorption capacities. The effect of change in parameters such as pH and ionic strength were evaluated.

2.3 Effect of pH

The amino groups on the surface of chitosan can be positively charged at low pH, and the charged surface may repel metal ions and prevent them from binding onto the adsorption sites. Furthermore, in the case that the amino groups are the binding sites, metals have to compete and replace the adsorbed proton in order for them to bind to the functional sites. As reported by Park et al. (1984), out of many cations only Cu^{2+} coordinated with chitosan at pH below 5.8, showing an adsorption band at 265 nm in a UV spectrum, because only copper competed strongly enough with protons for the active sites at low pH.

Hypothesis 4): Adsorption of Cu^{2+} and Cd^{2+} increases with increase of pH

Test: Adsorption of copper and cadmium at different pH by chitinous polymers with various DDA was studied.

2.4 Effect of sulfate on the adsorption

It was observed by Muzzarelli (1977) that conditioning of chitosan by H_2SO_4 decreased the sorbent's uptake capacity of many metals at pH 3 and pH 5. The reason for the reduction was not addressed. In contrast, adding $(NH_4)_2SO_4$ into the solution increased the total uptake. Similarly, Mitani et al. (1995) reported that sulfate stimulated the adsorption of Co^{2+} and Ni^{2+}. The reason for this improvement was not clear, only a few unproven speculations were made, such as an increase of the crystallinity or ionic exchange:

$$-NH_3^{+-}SO_4NH_4 + Me^{2+} = -NH_2Me^{2+} + NH_4^{+-}HSO_4 \qquad (2\text{-}1)$$

Hypothesis 5): Conditioning the polymer with H_2SO_4 stabilizes the polymer and fixes excess protons in the network, which repel the metal ions trying to diffuse in and reduce the adsorption.

Test: Stabilizing the polymer structure by H_2SO_4 or K_2SO_4 was tested by soaking the polymer in diluted HNO_3 solutions at pH 3; the total dissolved carbon was measured to estimate the extent of dissolution. Release of the proton from sulfuric acid conditioned polymers during the adsorption was monitored. Adsorption of Cu^{2+} at pH 6 was conducted using the same sample before and after conditioning with H_2SO_4 to determine whether the adsorption was still lower than the untreated chitosan.

Hypothesis 6): The improvement of the uptake caused by adding sulfate salt simultaneously is a result of increased permeability of the polymer under the elevated ionic strength and reduced surface charge.

Test: The trend of adsorption change with ionic strength variation was investigated using both nitrate and sulfate salts. Zeta potentials of the sorbent were measured with nitrate or sulfate added into the solution to verify that addition of sulfate reduced the surface charge.

Chapter 3

Materials and methods

All experiments used double deionized (DDI) water and ACS reagent grade chemicals. Metal stock solutions (purchased from VWR) with a concentration of 1000 ppm with 3% nitric acid were used as the standard solution for Atomic Absorption Analysis. Solutions used for the experiment were diluted from the stock solution with DDI water. 0.1 M HNO_3 and 0.1M NaOH were used to adjust the pH, and $NaNO_3$ solution was used for ionic strength control.

3.1 Preparation of sorbents

Freeze-dried Alaska king crab shells were crushed manually. The particle size fraction between 1-2 mm was sieved out for further processing.

(a) Acid-washed crab shell: the crushed crab shells were soaked in 50 g/L hydrochloric acid (HCl) at room temperature for 24 hr for decalcification following Muzzarelli's (1977) method. The solid: liquid ratio was 1:10 (w/v). The product was washed to neutral pH afterwards;

(b) Chitin: the acid-washed crab shells were heated in a 5% NaOH solution to 90° C for three times for 40min each to remove the proteins. The NaOH solution was renewed for each extraction. Chitin remained as product after being washed to neutral pH;

(c) Chitosan: Chitosan samples with different DDA were obtained by hydrolyzing chitin in concentrated NaOH solutions (10% to 40% (w/w)) at a temperature of 120° C for 120 minutes.

3.2 Determination of DDA

DDA was measured in this study in three different ways: potentiometric titration, Fourier Transform Infra-Red (FTIR) spectroscopy and proton-nuclear magnetic resonance (^{1}H-NMR) spectroscopy.

3.2.1 Potentiometric titration

Potentiometric titration was carried out on a Metrohm 719 titrator. 0.05g of chitosan sample was added into a 100 ml beaker containing 0.5 ml 1M HNO_3, and then the solution was diluted to a volume of 50 ml. After stirring for 20 minutes, the solution was titrated by 0.1 N NaOH.

3.2.2 ^{1}H-NMR spectroscopy

Previous research has shown that ^{1}H-NMR is a reliable method to directly determine the DDA of chitosan (Hirai et al., 1991). To obtain the ^{1}H-NMR spectra of low DDA chitosan, 10 mg of sample were dissolved in 2 mL 20% (wt./wt.) deuterium chloride (DCl), while for high DDA chitosan the same amount of sample was dissolved into 1.96 mL of D_2O and 0.04 mL of 20% DCl. The spectra were recorded on a 300 MHz ^{1}H-NMR (Varian-Mercury-300BB) spectrometer. Software (VNMR) was employed for data analysis. When 20% DCl was used as solvent, the peak of the acetyl proton was set to 1.85 ppm without adding any internal standard.

3.2.3 FTIR spectroscopy

Fourier transform infrared (FTIR) measurements were carried out using KBr discs prepared from a dried mixture of about 1 mg of the sample and 100 mg of KBr powder.

The FTIR spectrum was recorded on a Thermo IR100 spectrometer. DDA is measured by calculating the ratio of the absorbance of a probe band (PB), whose intensity changes with DDA related to the absorbance of a reference band (RB), whose intensity does not change with DDA. The intensities of the adsorption bands were determined based on the baseline method.

3.3 Determination of crystallinity

As stated in the introduction, the configuration of chitosan is based on numerous crystallites dispersed in an otherwise amorphous matrix. In this study, powder x-ray diffraction was applied to study the crystallographic properties of chitosan after fine grinding. The chitosan samples with DDA=42.3 were bought from Biosyntech Co. and other samples were made in the laboratory. The x-ray diffraction patterns were obtained on a wide-angle x-ray diffractometer (for $Ka_{1,Cu}$, radiation λ is 1.5405Å). The voltage was 40 kV and the current was 25 mA. The 2θ angle was scanned between 3° to 35°, and the counting time was 4 s at each step (0.01°). The crystallinity index was estimated using the equation based on the method proposed by Struszcyzyk (1987) and Focher et al. (1990):

$$\text{CrI}=\frac{I_{020}-I_{am}}{I_{020}}\times 100\% \qquad (3\text{-}1)$$

Where I_{020} =maximum diffraction pattern intensity (i.e. peak height) at $2\theta \approx 20°$ and I_{am} = amorphous diffraction pattern intensity at $2\theta \approx 16°$.

The crystallite size was calculated by using the Scherrer equation at $2\theta \approx 20°$:

$$B_r = \frac{k\lambda}{L\cos\theta} \qquad (3\text{-}2)$$

Where λ is the wavelength of the X-ray used, θ is the Bragg angle, L is the average crystallite size, and k is a constant assumed 1.0 (Suryanarayana and Grant, 1998). B_r is the remaining full width at half of maximum (FWHM), which is related to crystallite size and lattice strain and is obtained by subtracting the instrumental effect B_i from the observed width B_o ($B_r = B_o - B_i$).

3.4 Adsorption study

3.4.1 Selection of sorbents

Four different types of sorbents, namely raw crab shells, acid-washed crab shells, chitin and chitosan, were tested for their adsorption capacities for both $Cu^{2+}$and Cd^{2+}. Adsorption of metal ions was carried out by using biosorbents at a concentration of 0.2 g/L and metal solutions in the concentration range of 0-20 ppm in order to avoid precipitation. Continuous mixing was applied by magnetic stirring. The pH was controlled at 6 for $Cu^{2+}$and 7 for Cd^{2+} throughout the adsorption process by adding 0.1 N HNO_3 and 0.1N NaOH. This pH value was chosen to avoid sorbent dissolution at lower pH. $NaNO_3$ was added to control the background ionic strength at 0.01 N. Previous research (Mcafee et al., 2001; Chu, 2002) suggested that 12 hours was sufficient for equilibration. After 12 hours, the samples where filtered through a macrofilter (0.45 μm pore size).

3.4.2 Effect of pH on metal adsorption by chitosan

pH can be a controlling factor for the adsorption of metals because under acidic conditions, the fairly abundant protons compete with positively charged metal ions for the binding sites. Depending on the strength of interaction between chitosan and different metal ions, the extent of the pH effect should be different from metal to metal. Adsorption of $Cu^{2+}$and Cd^{2+} was studied using biomass at a concentration of 0.2 g/L and 20 mg/L metal solutions. Continuous mixing was applied by magnetic stirring. The pH was controlled at 4, 5, 6 or 7 throughout the adsorption process by adding 0.1N HNO_3 and 0.1N NaOH. $NaNO_3$ was added to control the background ionic strength at 0.01N.

3.4.3 Effect of sulfate conditioning

The chitosan sample was divided into two batches. One batch was used for metal adsorption after it was conditioned by H_2SO_4 or $(NH_4)_2SO_4$, and the other was used without conditioning. The pretreatment was done following Muzzarelli and Rochetti's method (1974) with slight modification. Accordingly, chitosan (1g) was introduced into about 100 ml of 0.1 M H_2SO_4 or 0.1 M $(NH_4)_2SO_4$ solution. After 8 hours stirring, the polymer was filtered out and washed till neutral. Adsorption of Cu^{2+} of 1-20 mg/L, using chitosan both with and without pretreatment was done at pH 6. The background electrolyte concentration equaled 0.01M achieved by adding $NaNO_3$ solution. The biomass was filtered out after the adsorption, and the filtrate was measured for both metal concentrations afterwards.

3.4.4 Effect of ionic strength

Adsorption of Cu^{2+} (concentration from 1-20 mg/L) was carried out with ionic strength (IS) equal to 0.001 and 0.01 respectively. The effect of $NaNO_3$ and K_2SO_4 as ionic strength control on the adsorption were studied separately. The particular effect of K_2SO_4 on the adsorption was also studied by using Cd^{2+} as the sorbent. The pH was 6 for Cu^{2+} and 7 for Cd^{2+} adsorption.

3.4.5 Determination of the amount of metal adsorbed

The initial and equilibrium concentrations of metal ions were determined by graphite furnace atomic adsorption spectrometry (Perkin Elmer AAnalyst 300). The uptake amount q (mg/g) was calculated from the mass balance for the respective heavy metal:

$$q = (C_0 - C_{eq}) \times V / M \qquad (3\text{-}3)$$

Where C_0, C_{eq}, V and M were the initial metal concentration (ppm), equilibrium metal concentration (ppm), volume of the solution (mL) and sorbent mass (g) respectively.

3.5 Stability study

Stability of the chitosan samples was tested by soaking the polymer in diluted HNO_3 solutions at pH 3 for 12 hours. Total Organic Carbon (TOC) of the filtrate after adsorption was measured on a Tekmar Dohrmann Apollo 9000 TOC instrument. The results were used to calculate the percentage of sorbent dissolution through equation 3-4:

$$Dissolution(\%) = \frac{TOC \times V / 12}{M \times [6 \times DDA + 8 \times (1 - DDA)] / [161 \times DDA + 203 \times (1 - DDA)]} \qquad (3\text{-}4)$$

Where TOC was the total organic carbon (ppm), 161 was the molecular weight of a D-glucosamine unit, 203 was the molecular weight of an acetyl-D-glucosamine unit, 12 was the atomic weight of carbon, DDA was the degree of deacetylation (%) and V was volume of the solution (mL) and M was sorbent mass (g).

3.6 Surface charge study

The zeta potential, which reflects the charge density on the surface, was determined here to quantify the change of surface charge when sulfate or nitrate was added into the solution. Chitosan samples were soaked in the solution with a concentration of 0.1 g/L for 12 hours to allow sufficient reaction with the salt added. The pH of the solution was controlled at pH 6 by adding 0.1N HNO_3 and 0.1N NaOH. The zeta potential was measured on a Brookheaven ZetaPlus analyzer.

Chapter 4

Measurement of DDA

There are three common ways to detect the DDA: nuclear magnetic resonance (NMR), Fourier transforms infrared (FTIR) and potentiometric titration. Each method will be discussed.

4.1 DDA measurement by NMR

Both solid-state ^{13}C-NMR and liquid-state ^{1}H- NMR were applied previously to study the DDA. Although NMR is expensive, it is believed to be the most accurate method for DDA measurement nowadays (Lavertu et al., 2003), and is used in the pharmaceutical industry as a standard method (Biosyntech Co.).

In this study, ^{1}H- NMR spectra were obtained. (Example spectra are shown in Fig. 4.1). Dividing the peak area for the acetyl group HAc, which possesses three hydrogen atoms, by three and the signal area H26 of the ring structure, which possesses six hydrogen atoms, by six, allows calculating the fraction of acetylated groups as (HAc/3)/(H26/6). Correspondingly, the DDA was calculated as:

$$DDA(\%) = \left(1 - \frac{\left(\frac{HAc}{3} \right)}{\left(\frac{H26}{6} \right)} \right) \times 100 \qquad (4\text{-}1)$$

The DDA calculated from the NMR method was used as the standard DDA. The accuracy of FTIR and potentiometric titration measurement was evaluated based on comparison to that standard DDA.

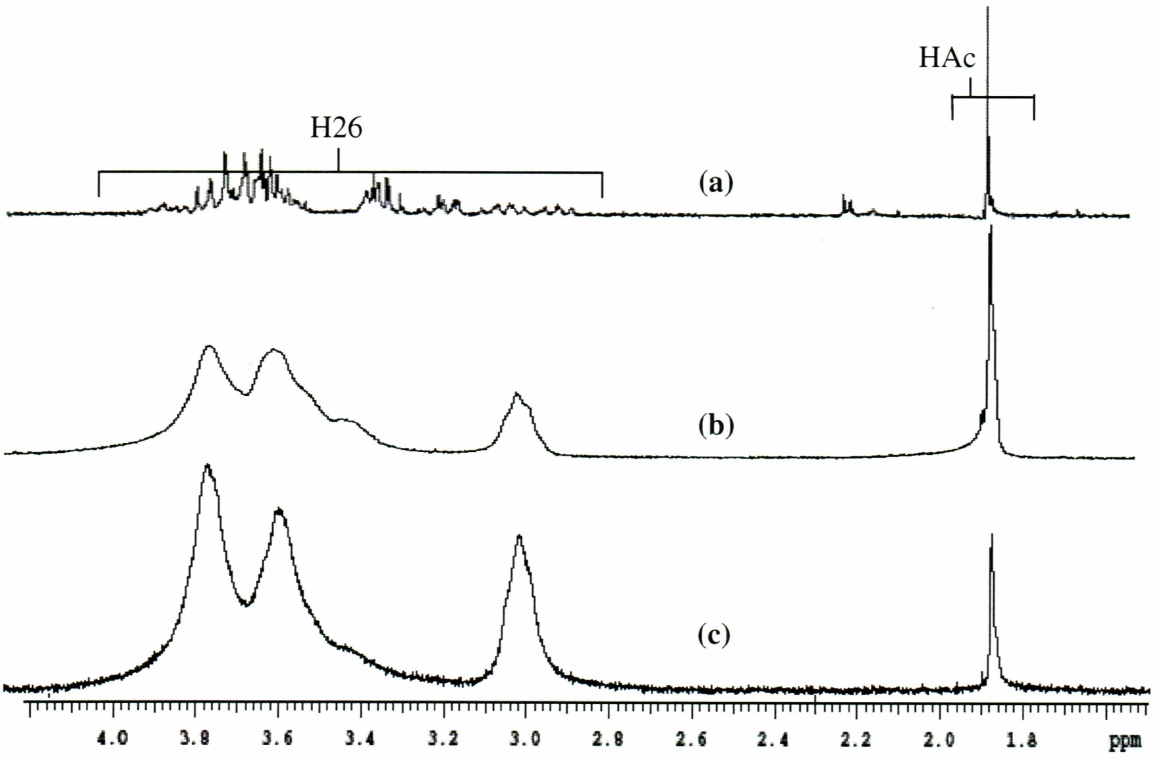

Fig. 4.1 ^{1}H-NMR spectra of chitosan with (a) DDA~13.4, (b) DDA~43.6 and (c) DDA~90.8

4.2 DDA measurement by FTIR

Using FTIR to determine DDA is easy, fast and accurate only if the right PB, RB and baselines are chosen. DDA is measured by calculating the ratio of the absorbance of a probe band (PB), whose intensity changes with DDA, with the absorbance of a reference band (RB), whose intensity does not change with DDA. The intensities of the adsorption bands are determined based on the baseline method. This problem has been widely discussed with numerous baselines and calculations proposed.

As shown in Fig.4.2, the preferred PB was the absorption of amide I (carbonyl stretching) at 1665 cm^{-1} and/or amide II (NH bending) at 1560 cm^{-1}; while the RB was

chosen from the absorption of OH stretching at 3450 cm^{-1} and the CO stretching in the range of 1075 cm^{-1} to 1025 cm^{-1} (Duarte et al., 2002 and Shigemasa et al., 1996).

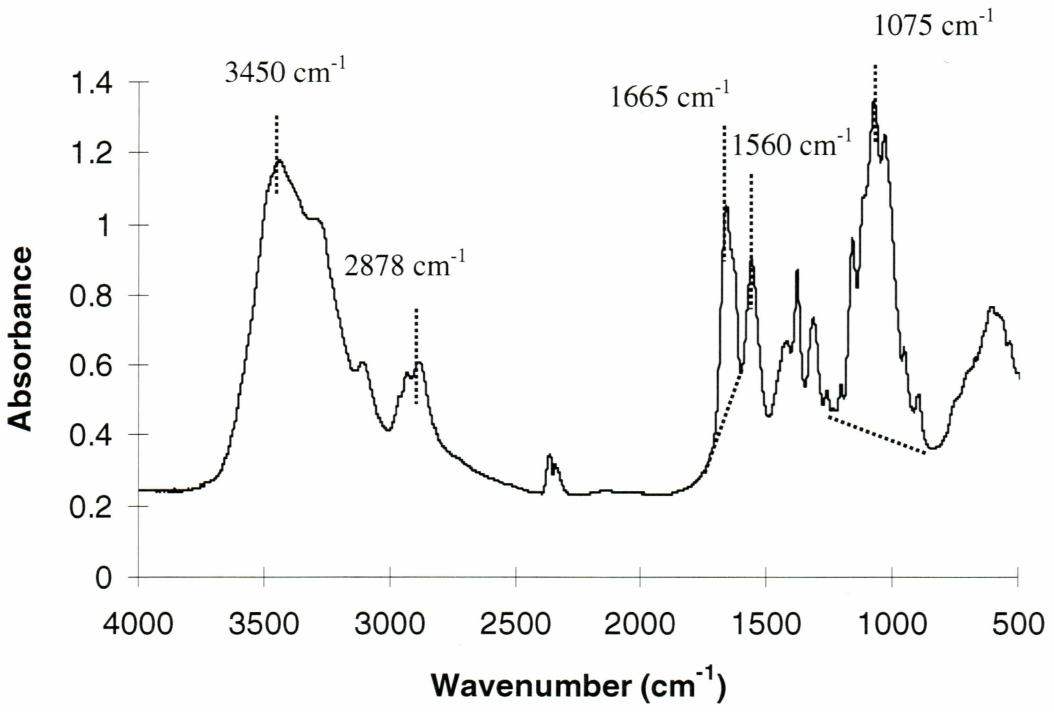

Fig. 4.2 Peak assignment for FTIR spectrum of chitosan

The transient of OH stretching at 3450cm^{-1} was chosen as the RB in some studies (Domszy and Roberts, 1985; Baxter et al., 1992; Sabnis and Block, 1997), which is not suggested by the current author because it is affected by the intense NH stretch at 3269 cm^{-1}. Moreover, the OH stretching of water (due to any remaining moisture content in the sample), which is in the range 3570 cm^{-1} to 3200 cm^{-1}, covers the RB peak A3450. Instead, at least 4 bands observed in the range of 1075 cm^{-1} to 1025 cm^{-1}, representing the OC stretch due to ring COH, COC, CH_2OH groups, are expected to be a good RB, since the intensity of these groups won't change with the DDA. As far as the PB is concerned, the absorption of amide I (carbonyl stretching) at 1665 cm^{-1} is a preferred PB compared

to amide II (NH bending) at 1560 cm^{-1} because for high DDA samples, the band shifts to 1597cm^{-1} after the resonance between C=O and N is destroyed, which means the peak at 1597 cm^{-1} no longer represents the amide group, but rather the amino group. In contrast, the amide I (carbonyl stretching) at 1665 cm^{-1} remains at the same position as DDA changes with its relative strength decreasing with the increase of DDA.

In this study, the absorption of the amide carbonyl stretching at 1665 cm^{-1} was chosen as the PB, and the absorption of CO stretching at 1075 cm^{-1} was chosen as the RB. From Fig. 4.3, it is very clear that the PB decreases as DDA increases while the RB remains the same throughout the DDA variation.

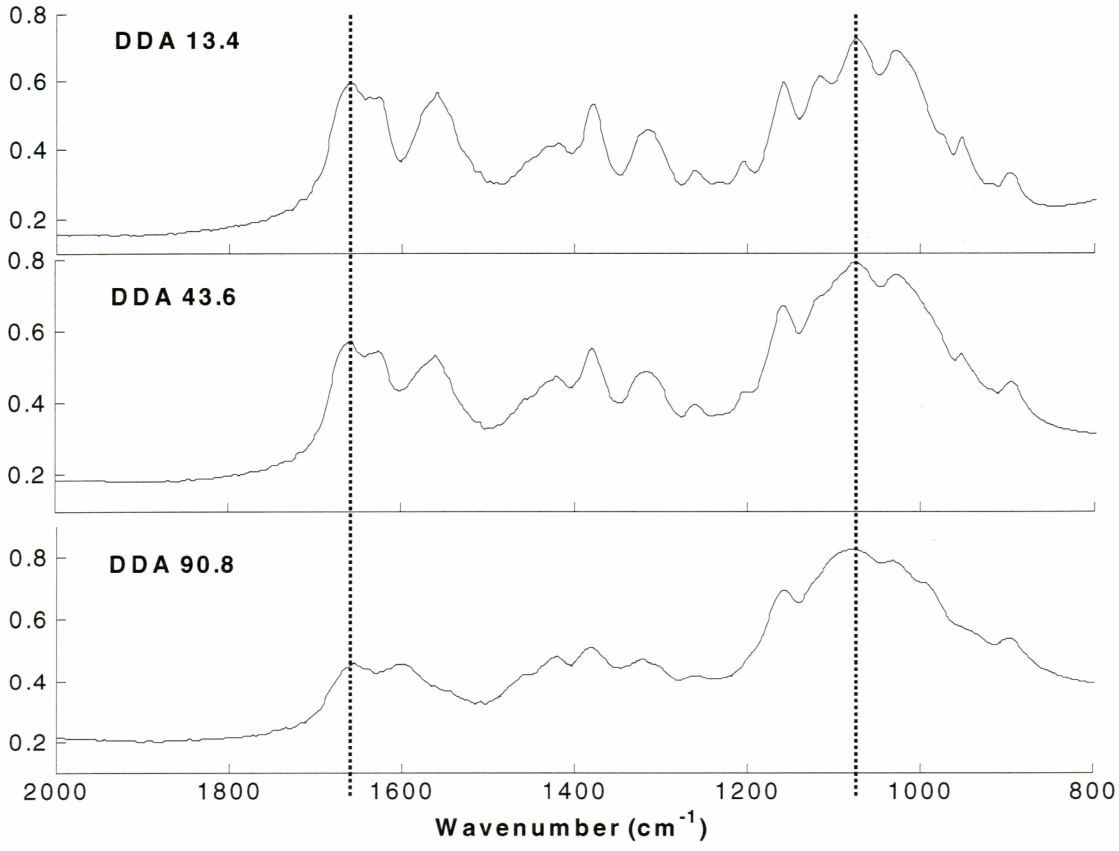

Fig. 4.3 Variation of peak intensities with change of DDA

After certain peaks are chosen for PB and RB, the DDA cannot be calculated by simply taking the peak ratio of PB over RB, because the baselines chosen might not be the real baselines and the effect of peak overlap can not be totally avoided in this baseline method. Previous research has shown that determination of the DDA by using the NMR calibrated FTIR spectroscopy can solve this problem. The peak ratio was plotted against the NMR DDA as shown in Fig 4.4. The linear relationship between the NMR DDA and the FTIR peak ratio indicated that FTIR can be used for DDA measurement. The function developed for FTIR DDA calculation based on the linear relationship is expressed as:

$$DDA = 115.7 - 140.85\frac{A1655}{A1075} \qquad (4\text{-}2)$$

Where A1665 is the PB and A1075 is the RB.

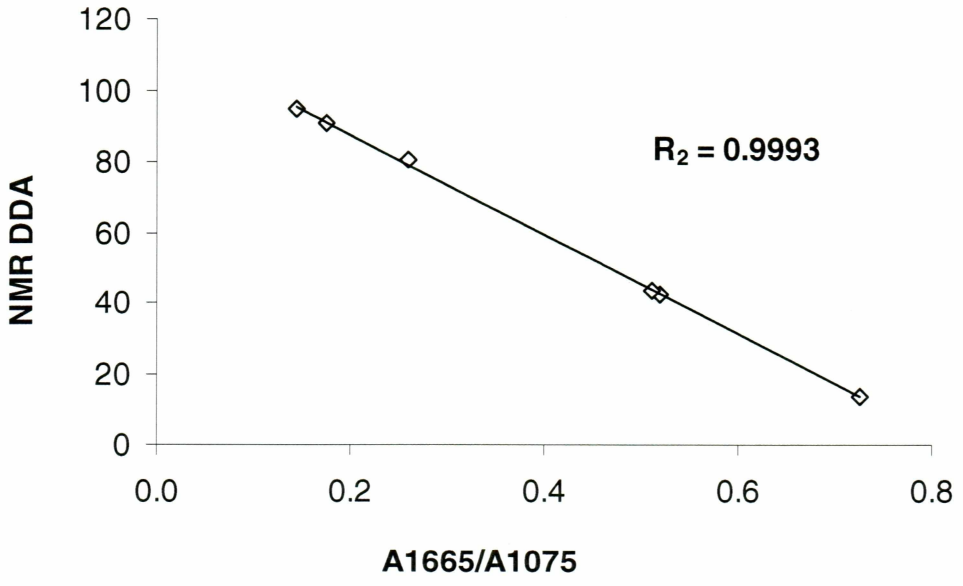

Fig. 4.4 Linear relationship between the NMR DDA and FTIR peak ratios with the peak at 1665 cm^{-1} as PB and the peak at A1075cm^{-1} as RB

A comparison of FTIR DDA calculated using the function developed in this study with the NMR DDA is provided in table 4.1, which shows the FTIR DDA matches with the NMR DDA fairly well.

Table 4.1 Comparison of FTIR DDA with NMR DDA

Sample ID	FTIR DDA (%)	NMR DDA (%)
H10-120	13.38	12.41
H20-120	18.28	19.89
H30-120	43.69	40.54
H40-120	90.84	94.05

Note: Sample ID represents the hydrolysis conditions, for example: 10% H10-120 means sample was treated with 10% (w/w) NaOH at120° C for 120 minutes.

4.3 Potentiometric titration

Potentiometric titration has been used as a technique for DDA measurement by some researchers (Mima et al., 1983 and Rhazi et al., 2000). In this study, its reliability was discussed in comparison with the NMR method. The potentiometric titration curves of chitosan samples with DDA=13.4 and DDA=43.6 are shown in Fig. 4.5, along with the titration of the acid background.

From the titration curve the DDA was calculated based on the assumption that all the deacetylated sites are titrable. Those sites were initially protonated at low pH. During the titration, the protons in the solution were consumed by the added NaOH, then the protons bonded on the sites were released to the solution to reestablish the equilibium: ($R\text{-}NH_3^+ \longrightarrow R\text{-}NH_2 + H^+$). That was where the first inflection of the curve appear. The

more NaOH was added into the solution, the more protons were released from the binding sites to the solution. After all the previously bound protons were consumed, the change of pH was only controlled by the addition of NaOH. That point corresponds to the second inflection in the curve.

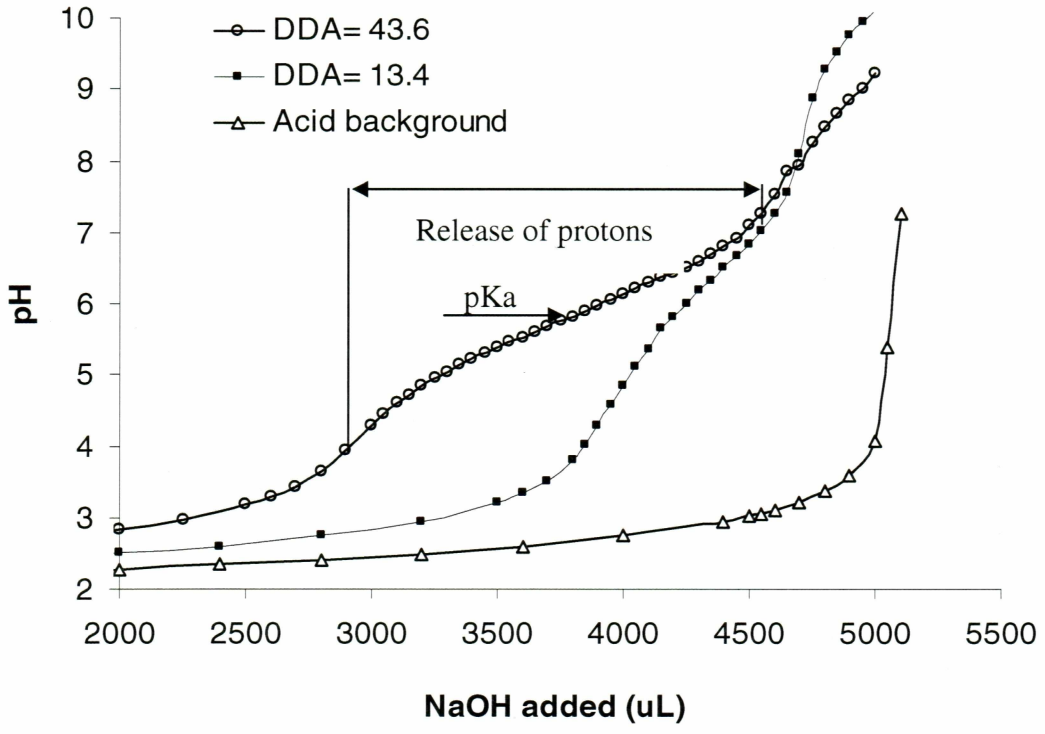

Fig. 4.5 Potentiometric titration of chitosan

The amount of base consumed between the first and the second inflection is considered to be equal to the the amount of amino groups which can be charged, in other words, deacetylated. DDA is calculated using equation 4-3 (Muzzarelli, 1977):

$$\mathrm{DDA}=161\times C\times(v_2-v_1)/W \qquad (4\text{-}3)$$

Where 161 is the molecular weight of a D-glucosamine unit; v_1 and v_2 are the consumed NaOH volumes at the two inflection points; C is the concentration of NaOH and W is the sample weight. The calculated DDA is listed in Table 4.2 along with the DDA obtained though NMR methods.

Table 4.2 Comparison of DDA obtained through potentiometric titration and NMR

Sample ID	NMR DDA (%)	Titration DDA (%)
H10-120	12.41	11.3
H20-120	19.89	14.6
H30-120	40.54	28.2
H40-120	94.05	85.3

The DDA obtained though the potentiometric titration matches some DDA values measured by NMR reasonably well (especially compared to the FTIR approaches of other authors as listed in Table 4.1) but shows a big discrepancy for the H30-120 sample, which means the previous assumption that the all deacetylated sites are titrable is highly questionable for medium DDA. To understand this, the configuration of the polymer has to be studied. As stated in the introduction, the stucture of chitosan is partly crystalline with some of its chains organized into ordered ranges called crystallites and others randomly arranged to form an amorphous matrix. The crystallite regions were believed to be impermeable to solutions under normal circumstances (Comyn, 1985). It is plausible to imagine that with high crystallinity and large crystallite size, the permeability of the polymer will be low. Thus the active sites entrapped deep inside the particle are hardly titrable.

The other issue that needs to be addressed is the dissolution of the polymer. It is well known that chitosan with DDA>50% is soluble in diluted acid, while chitin with DDA<50% does not dissolve significantly. In the current case, the H40-120 dissolved nearly completely in the diluted HNO_3 at pH 2.5 before titration by NaOH, so it is reasonable to trust that the total titrable sites represent the total amount of amino groups. However, for the H10-120, H20-120 and H30-120 samples, the question is do they dissolve and how much do they dissolve? In the process of heterogeneous deacetylation, as in this case, solid chitin particles were soaked in the base solution. Thus, it is expected that the deacetylation starts from the surface, and then proceeds into the particle through the fractures "eating up" the crystallite and enlarging the deacetylated amorphous area. Since it is believed that the intra- and intermolecular hydrogen bonds in the crystalline regions are responsible for the resistance of chitin/chitosan to swelling or dissolving (Guo et al., 2002), the amorphous area can dissolve. If the entire deacetylated outer layer and the amorphous region of the particle dissolves into the solution before titration, the titratable sites will still equal the total amount of sites.

Partial dissolution was proven to occur in the chitin sample with DDA=42.3. After being stirred in acid at pH 2.5, it was observed in the x-ray diffraction pattern (Fig 4.6) that the amorphous hump above the baseline was reduced. Quantitatively, the CrI increased from 64.8 to 73.9. At the same time, the FTIR DDA decreased from 42.3 to 36.8 after the dissolution, which meant that some of the deacetylated amorphous region dissolved but not all.

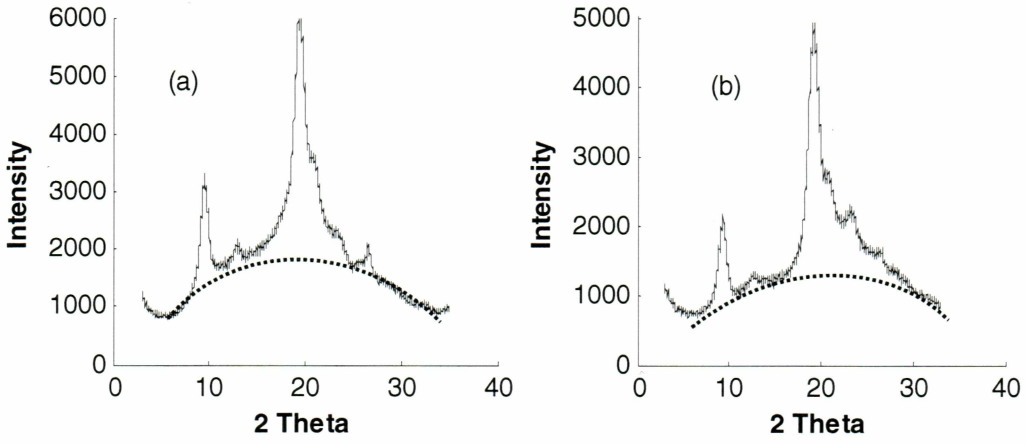

Fig. 4.6 XRD pattern for selected samples (a) DDA=42.3 CrI=64.8, before dissolution, (b) DDA=36.8 CrI=73.9, recovered after partial dissolution of sample (a)

After the dissolution, the total titrable sites consist of the amino groups on the solid surface and the amino groups on the dissolved chains in the liquid state. The amino groups entrapped in the crystallite are still not all accessible since the DDA gained by potentiometric titration was consistently lower than the true DDA obtained on NMR.

Furthermore, the observed discrepancy was relatively small at both the high DDA end and the low DDA end, but larger in the middle DDA range. This can be explained by the fact that the deacetylation starts from surface and both the CrI and the crystallite size decrease with DDA increase (Fig.4.7).

Therefore, for the low DDA sample, all amino groups were expected to be distributed near the surface and titrable; while for the high DDA sample, the crystallites were so small that the material dissolved nearly completely in the acid solution. Thus, all the amino groups on the surface of the crystallite and in the amorphous area were exposed for titration. For the middle range DDA sample, more than the outer surface of

the particle was deacetylated, but the crystallites were still big enough to maintain a low permeability, so the total titrable sites are much lower than the amount of amino groups throughout the material.

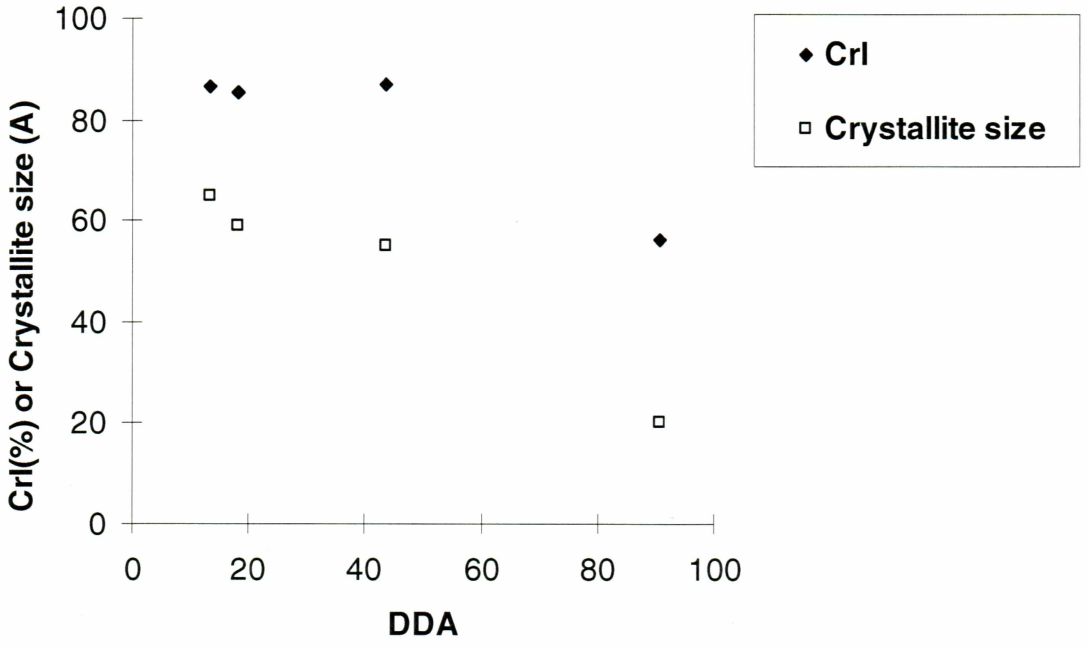

Fig. 4.7 Change of crystallinity index and crystallite size with DDA

Chapter 5

Adsorption of Cu (II) and Cd (II)

In this chapter, six different sorbents derived from crab shells, namely acid-washed crab shell, chitin with DDA=13.4, chitin with DDA=43.6, chitosan with DDA=80.7, K_2SO_4 conditioned chitosan with DDA=80.7, and H_2SO_4 conditioned chitosan with DDA=80.7 were tested individually for their adsorption capacity for Cu^{2+} and Cd^{2+}. The influence of other factors such as pH, ionic strength and co-existent SO_4^{2-} anions was also studied. Visual-MINTEQ was employed to calculate the phase distribution of the metal ions at the highest concentration used in this experiment and at the highest pH to ensure that no precipitation occurred during the adsorption.

5.1 Investigation of the optimum sorbent

Crab shell along with all its derivatives, namely acid washed crab shell, chitin and chitosan have been used as sorbents for either metal ions or metal oxyanions (Kim and Park, 2001; Niu and Volesky, 2003). However, since the cost of the sorbent varies, it is necessary to understand how and why each of those sorbents works and compare their adsorption capacity for the target metal. Cu^{2+} was first used to test the adsorption capacity of the sorbents. The resulting adsorption isotherms are plotted in Fig. 5.1. The plot shows that raw crab shell does not bind with Cu^{2+} and chitosan with higher DDA has a higher adsorption capacity for Cu^{2+}, which confirms our hypothesis that the amino group is more effective than the acetyl amine group for Cu^{2+} adsorption. The uptake capacity improved by more than one third when the DDA increased from 13.4 to 43.6, but increased less significantly for further DDA increase from 43.6 to 80.7. This

observation was consistent with some previous results. For adsorption of mercury and copper by chitosan with different DDA, Kurita et al. (1977) found that the maximum removal of both metals was not directly proportional to the amino group content. In the DDA range higher than 50%, the adsorption capacity of the sorbent was increased only slightly by further deacetylation. Kim et al. (2001) reported that both the adsorption of dye and Cr (IV) increased with an increase of DDA. However, the equilibrium adsorption capacity for samples with DDA=46.8% and DDA=36.3%, differenced only slightly (less than 0.5 mg/g). The reason that the adsorption capacity does not increase significantly after the DDA exceeded 40% could be related to the binding site distribution inside the polymer and the permeability of the material.

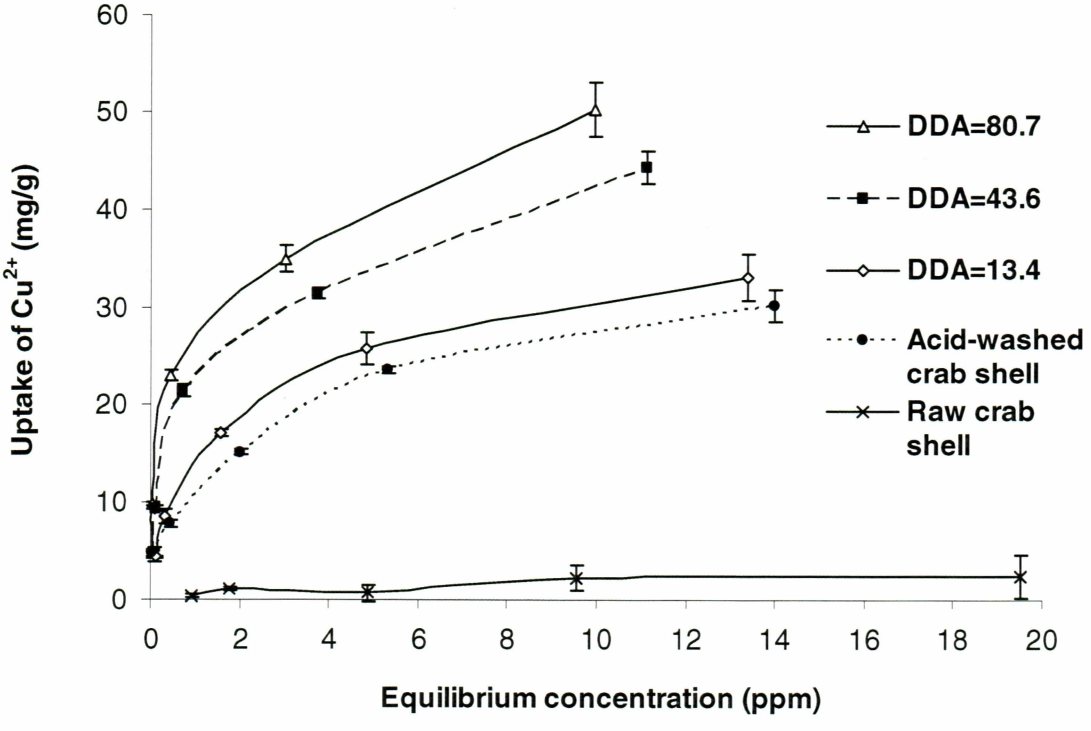

Fig. 5.1 Adsorption isotherms for Cu^{2+} by raw crab shell, acid-washed crab shell, chitin and chitosan with different DDA at pH 6 and IS 0.001

It is a little surprising to notice that the acid-washed crab shell showed a fairly good adsorption capacity, because the acid wash removes only $CaCO_3$ and the remaining chitin micro-fibers are embedded in a six strand protein helix, as occurs naturally. This protein layer would present a diffusional barrier for heavy metal ions. A schematic sketch was provided by Kristbergsson et al., (2003) to demonstrate the structure (Fig.5.2).

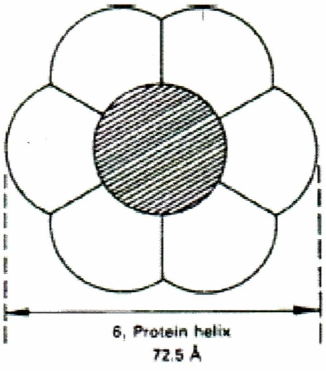

Fig. 5.2 Chitin micro-fiber embedded in protein matrix (Kristbergsson et al., 2003)

Since the chitin fibers are not directly in contact with the solution, it is likely that protein plays a role in metal binding. This appears to be especially true for the adsorption of Cd^{2+}. As shown in Fig. 5.3, the uptake of Cd^{2+} by the high DDA sample is higher than that for the low DDA sample, which again confirms the hypothesis that amino groups are superior to amide groups for metal binding. Acid-washed crab shells, which had not been through the deacetylation process, had very low DDA, thus the uptake by acid washed crab shell is much higher than expected. Additionally, the adsorption isotherm of the acid-washed crab shell is clearly different from those of the chitinous sorbent, which is a clear sign that something else rather than chitin/chitosan binds with the metal ion. According to the protein and chitin structure shown in Fig. 5.2, the active component of

this sorbent is highly suspected to be protein. More research is needed in the future to determine why the protein has higher affinity to Cd^{2+} than chitinous material.

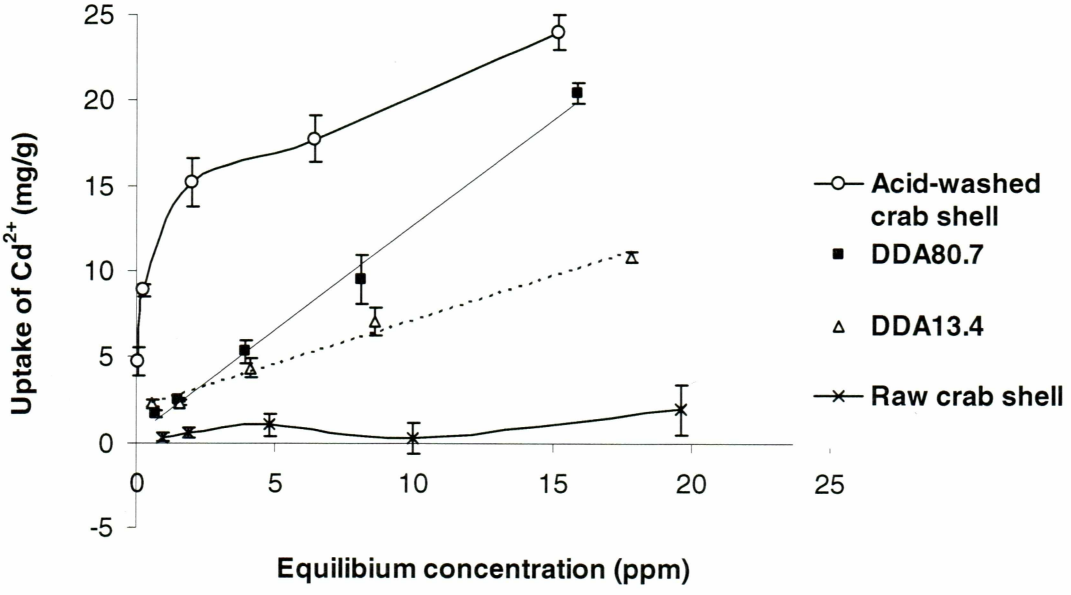

Fig. 5.3 Adsorption isotherm for Cd^{2+} by acid-washed crab shell, chitin and chitosan with different DDA at pH 7 and IS 0.001

By comparing Fig. 5.1 and Fig. 5.3, the uptake of Cd^{2+} by the same sorbent is always lower than that of Cu^{2+} in the isotherm study. Furthermore, the isotherm shape for the chitin with DDA=13.4 and chitosan with DDA=80.7 are very close to a straight line in the experimental concentration range. This indicates that the maximum uptake capacity of chitinous polymer could be significantly higher than the highest uptake shown in Fig. 5.3, and might even exceed the maximum uptake capacity for the acid-washed crab shells, for which the isotherm had already flattened out. However, the isotherm could not be extended to higher Cd^{2+} concentration due to potential precipitation. Stepwise addition of Cd^{2+} could be considered in future experiments to estimate the maximum uptake.

5.2 pH effect

It is well known that the surface charge distribution on the sorbent is determined by the pH value of the solution (equation 5-1) with most sites protonated at low pH. Thus, the metal ions have to be competitive and able to replace the adsorbed proton in order for them to bind to the protonated sites (equation 5-2), otherwise only the unprotonated sites are functional for metal adsorption (equation 5-3):

$$R\text{-}NH_2 + H^+ \longrightarrow R\text{-}NH_3^+ \qquad (5\text{-}1)$$

$$R\text{-}NH_3^+ + Me^{2+} \longrightarrow R\text{-}NH_2\text{-}\,Me^{2+} + H^+ \qquad (5\text{-}2)$$

$$R\text{-}NH_2 + Me^{2+} \longrightarrow R\text{-}NH_2\text{-}\,Me^{2+} \qquad (5\text{-}3)$$

The adsorption of Cd^{2+} at different pH values was studied using the chitin sample with DDA=13.4 as the sorbent, to avoid dissolution of the sorbent at low pH. The experimental results are shown in Fig. 5.4, which reveals that pH has a significant influence on the adsorption of Cd^{2+}. According to Fig. 5.4, there is no adsorption observed when the pH is below 5, and the uptake increases with increasing pH. Comparison between the initial concentration of Cd^{2+}, which is 20 mg/L or 1.79×10^{-4} mol/L, with the proton concentration at pH 5, which is 10^{-5} mol/L, suggests that H^+ is preferred over Cd^{2+} in the affinity sequence for this sorbent.

The adsorption of Cu^{2+} by this sorbent showed the same trend for varying pH (Fig. 5.5). The experiment was conducted with an initial Cu^{2+} concentration of 20 mg/L (3.15×10^{-4} mol/L). Little adsorption was observed at pH 4, while significant uptake appeared at pH 5. At pH 6, the adsorption of Cu^{2+} is three times higher than the adsorption of Cd^{2+}.

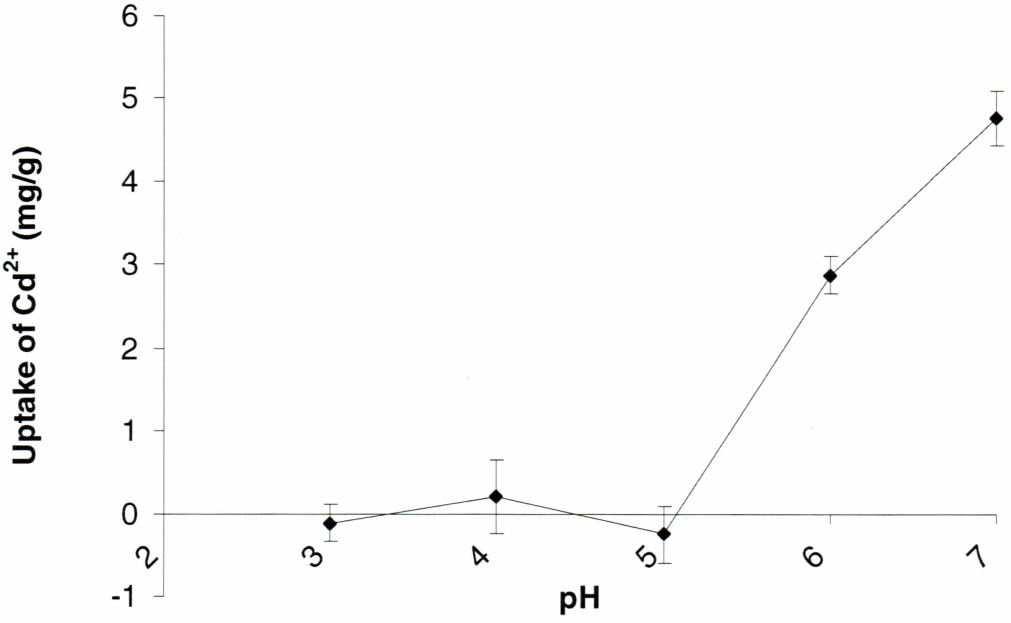

Fig. 5.4 Effect of pH on the adsorption of Cd^{2+} by chitin with DDA=13.4

From Fig. 5.5 the adsorption by DDA=80.7 is higher than the adsorption by DDA=13.4 along the pH range from 4-6. One certain reason is that the sample with high DDA has a higher amount of functional groups to bind with the metal. Another reason might be that the swelling of the polymer's network at low pH is more pronounced for the high DDA sample, causing a loser network, which leads to more binding sites becoming available. At the same time, the pH for the micro environment inside the network should be higher than the pH of the solution, because of the consumption of protons by the functional sites; thus, more Cu^{2+} adsorb. H_2SO_4 conditioned chitosan with DDA=80.7 behaved much like the sample with DDA=13.4 in the low pH range, showing low uptake, but the reason is suspected to be related to the excess protons enclosed in the network during the conditioning, which is discussed in the following section, instead of

less swelling. When the pH rose to 6, the uptake by the unconditioned chitosan and the conditioned one are almost the same.

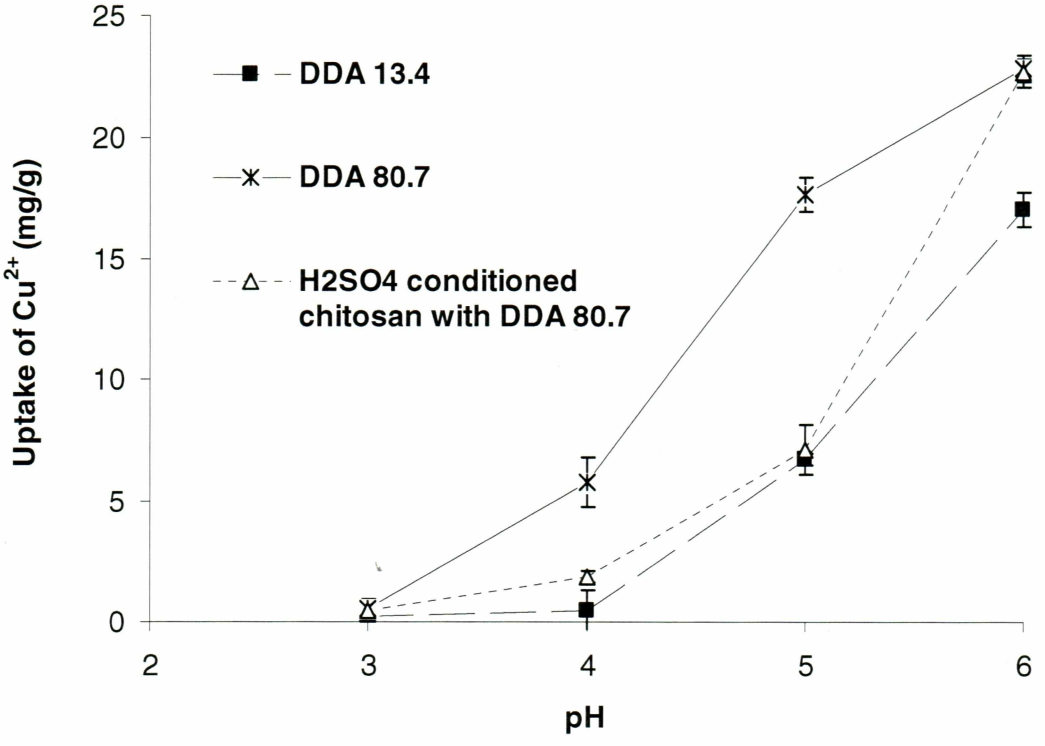

Fig. 5.5 Effect of pH on the adsorption of Cu^{2+}

5.3 Effect of sulfate conditioning

It was previously suggested by Muzzarelli and Rochetti (1974) that conditioning chitosan with SO_4^{2-} could change its affinity to metal cations. He observed results similar to those shown in Fig. 5.5 in that the H_2SO_4 conditioned chitosan was less efficient than unconditioned chitosan as a collecting agent for metal cations, but the $(NH_4)_2SO_4$ conditioned chitosan together with 0.1M $(NH_4)_2SO_4$ added in the solution showed enhanced adsorption for all the tested cations, such as Cr^{3+}, Mn^{2+}, Fe^{3+}, Ni^{2+}, Cu^{2+}, Zn^{2+} and Hg^{2+}. The author did not explain why conditioning the sorbent with H_2SO_4 reduced

the adsorption, but suggested that the enhancement of chitosan capacity in sulfate solution may have originated from ion exchange and a novel crystallinity induced in the polymer by sulfate.

To understand why conditioning reduced the adsorption in Muzzarelli's experiment, an experiment was set up to monitor the pH change during adsorption of Cu^{2+} (concentration ranged from 1 ppm to 20 ppm); pH was adjusted to 6 initially and ionic strength (IS) was controlled at 0.01 by adding $NaNO_3$. After 7 hours adsorption, the pH was recorded and plotted against the initial concentration of Cu^{2+} in Fig. 5.6. During the adsorption, the replacement of H^+ by metal ions should cause a decrease of pH; at the same time, chitosan swells in the solution, leading to more and more amino groups exposed. This process consumes protons and causes the pH to rise; the DDA 13.4 and DDA80.7 samples were both originally in the deprotonated state resulting from the basic medium of deacetylation, and therefore able to bind protons. The total pH change is the sum of the two processes and can be either positive or negative, depending on the properties of the sorbent as well as the amount of sorbent in the reaction. For the samples with DDA=13.4 and DDA=80.7, when the copper concentration was low, the pH change was positive, which indicated that the protons consumed during the swelling of the sorbent exceeded the protons replaced by Cu^{2+} during the adsorption. pH rose more for the high DDA sample because it swelled more and had more functional groups that could be protonated. As the initial copper concentration increased, the protons released from the sorbent overcame the consumption of protons for protonating amine groups exposed by swelling. Thus the pH dropped below the initial pH 6. When using the DDA=80.7

sample as sorbent, the pH dropped more than when using the DDA=13.4 sample, because there were more binding sites on the high DDA sorbent, which were previously occupied by protons and then released during adsorption of Cu^{2+}. The pH change was generally negative in the case of using H_2SO_4 conditioned chitosan as sorbent because a large quantity of H^+ was attached on the amino groups in the network during the conditioning process and released during the adsorption.

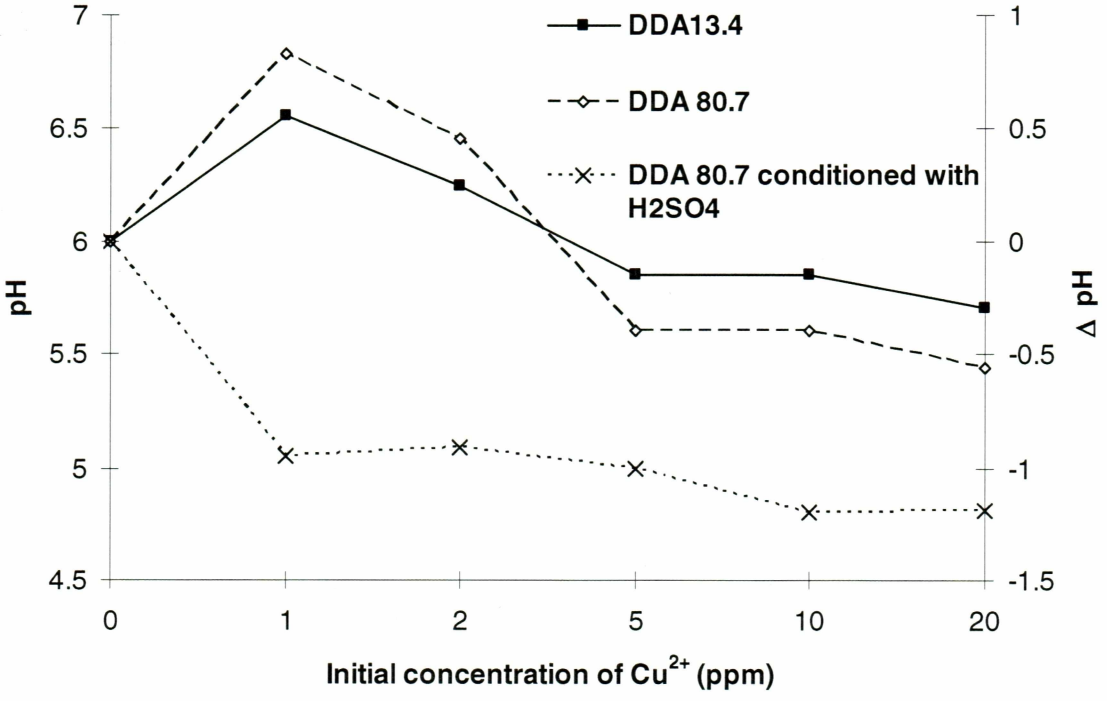

Fig. 5.6 pH of the adsorption solution after 7 hours' reaction with initial pH=6

The release of protons from sulfuric acid conditioned polymer during the adsorption of Cu^{2+} is more obvious if the amount of protons released is plotted against the initial concentration of Cu^{2+} for the above experiment, as shown in Fig. 5.7.

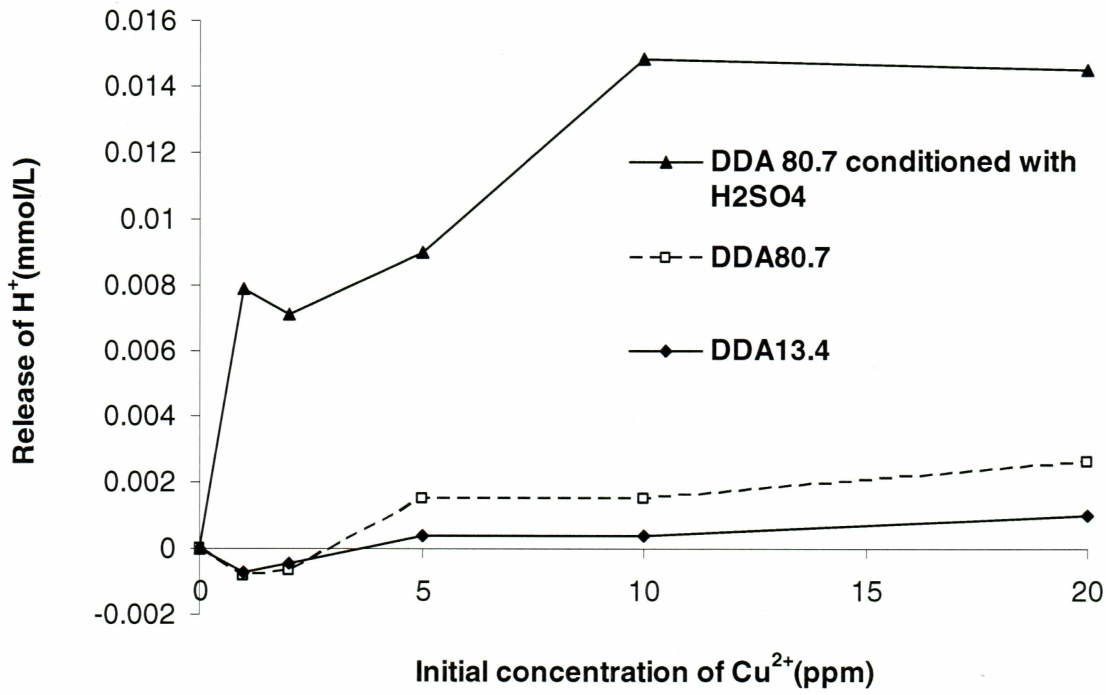

Fig. 5.7 Release of protons during the adsorption of Cu^{2+} by various sorbents

It is worthwhile to notice that all of Muzzarelli's experiments were conducted in an acidic environment with pH 3 and pH 5, in which case the protons binding with the amino groups inside the network could not be released by replacement of Cu^{2+} because the micro environment for H_2SO_4 conditioned chitosan was always acidic. As stated above, the uptake increases as pH increases; the extra protons remaining in the network might be the reason that conditioning with H_2SO_4 weakened the uptake. This low uptake of sulfuric acid conditioned chitosan compared to unconditioned chitosan is also shown in Fig. 5.5 at pH<6.

When the experiment was conducted at pH 6, as in this research, the protons in the conditioned polymer were released easily since OH^- ions were constantly provided to keep the pH at 6, and during the adsorption the deprotonated active sites were reoccupied

by the metals. Under this circumstance, the adsorption capacity of H_2SO_4 conditioned chitosan was quite similar to that of the unconditioned chitosan as shown in Fig.5.8.

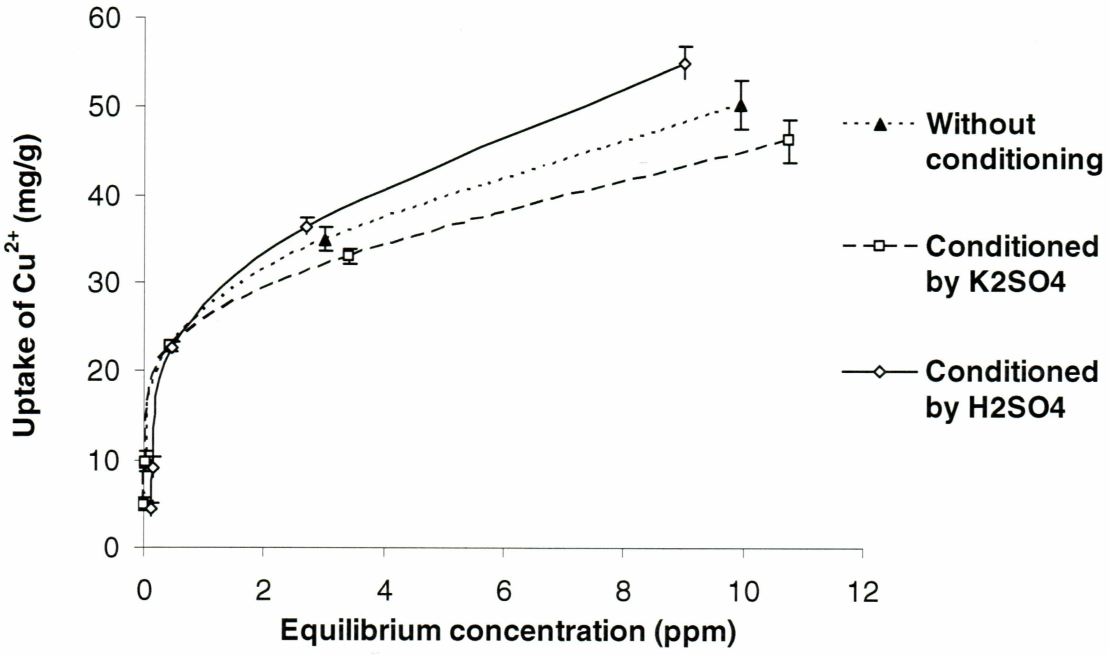

Fig.5.8 Adsorption isotherm for Cu^{2+} by chitosan with DDA=80.7, chitosan with DDA=80.7conditioned by K_2SO_4 and chitosan with DDA=80.7 conditioned by H_2SO_4 at pH 6

However, this does not mean conditioning with H_2SO_4 has no effect on the polymer network. It was reported that SO_4^{2-} could react with the amino groups in chitosan (Muzzarelli, 1977). In the process of conditioning by H_2SO_4, the network expanded at high ionic strength (as discussed in the following chapter) and the structure might be crosslinked and remain expanded after washing with water. Some of the exposed functional groups were occupied by H^+ and some by SO_4^{2-}. The attached protons could then be replaced by the metal during the adsorption. The total number of accessible

functional sites may increase because of the expansion and decrease at the same time because of SO_4^{2-} binding. It seems from Fig. 5.8 that the two effects compensate each other to a large extent and the overall influence was small.

The K_2SO_4 conditioned polymer showed slightly lower uptake than the H_2SO_4 conditioned one. That was possibly because during conditioning by K_2SO_4 the network expanded but might not have remained expanded after washing with water because no crosslinking took place in this case, which was verified by testing the solubility of the conditioned polymer as discussed below.

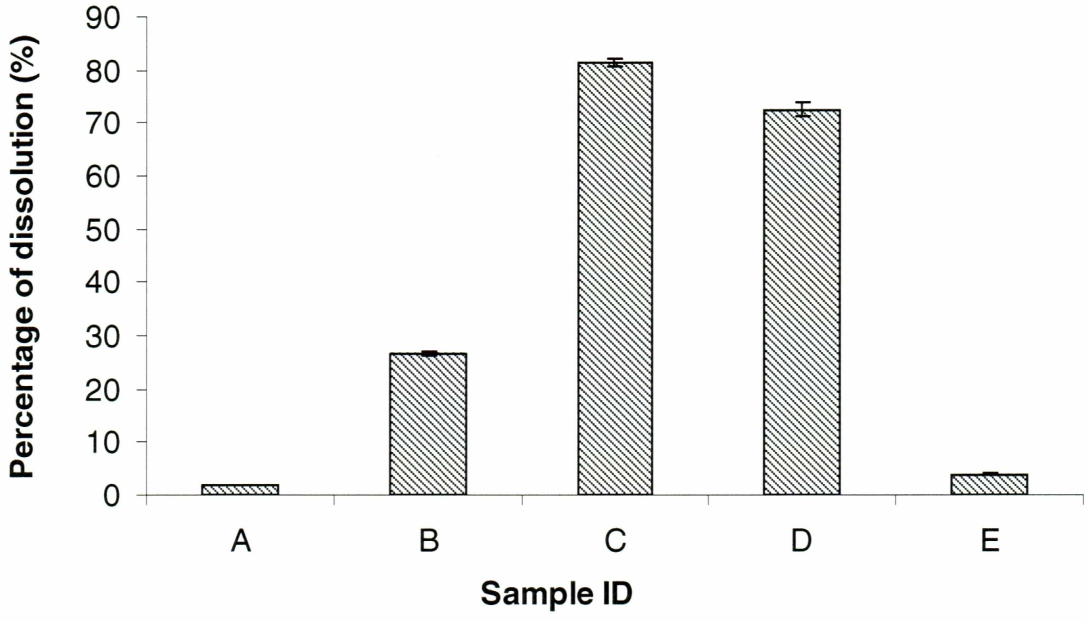

Fig. 5.9 Estimate of dissolution for chitinous samples at pH 3 and IS 0.01.

(A) Chitin with DDA=13.4, (B) Chitin with DDA=43.6, (C) Chitosan with DDA=80.7, (D) Chitosan with DDA=80.7 pretreated with K_2SO_4, (E) Chitosan with DDA=80.7 pretreated with H_2SO_4

Since cross-linking increases the level of stability of the polymer in acids, investigation of the dissolution behavior of the sorbent before and after the conditioning might reveal more about the structure change. It is well known that chitosan with DDA>50 is soluble in most inorganic acid and diluted mineral acid. Actually, as suggested in the previous chapter, part of the deacetylated regions of chitin with DDA< 50 is soluble also. Fig. 5.9 demonstrates that the extent of dissolution depends on the sample DDA: High DDA samples dissolve more under the same circumstances. However, conditioning the chitosan with H_2SO_4 can stop the dissolution. Chitosan conditioned with 0.1 M K_2SO_4 dissolved 72%, while the same sample pretreated with 0.1 M H_2SO_4 dissolved only 4%, which implies that SO_4^{2-} alone can not bridge two charged sites and crosslink the polymer. It is the binding of both H^+ and SO_4^{2-} that holds the polymer together. Since K^+ binds much less with amino groups than H^+, we can assume that no significant attraction force between positively charged sites and negatively charged sites is created when conditioning with K_2SO_4 at pH 6. Thus, no crosslinks are formed and the conditioned polymer is still soluble.

Since K_2SO_4 does not crosslink the polymer, the structure shrinks again after washing with water and made the extra functional sites unavailable. That is why the K_2SO_4 conditioned polymer showed lower uptake than the one conditioned by H_2SO_4. This result also indicates that the increase in metal uptake observed by Muzzarelli and Rochetti (1974) may be not caused by the $(NH_4)_2SO_4$ conditioning, but rather caused by the 0.1M $(NH_4)_2SO_4$ added into the solution. (These two treatments were performed

simultaneously and not investigated independenly) during the adsorption. This idea is discussed in the following section.

5.4 Effect of ionic strength and coexisting sulfate anion

According to the double layer model, if the surface and the sorbate are oppositely charged, the adsorption should either not be affected by the ionic strength significantly (inner sphere complex); or should decrease as the ionic strength increases (outer sphere complex) (Stumm, 1992). In this study, however, it was observed that adsorption increased with the ionic strength and the effect of sulfate was more pronounced than the effect of nitrate (as shown in Fig. 5.10).

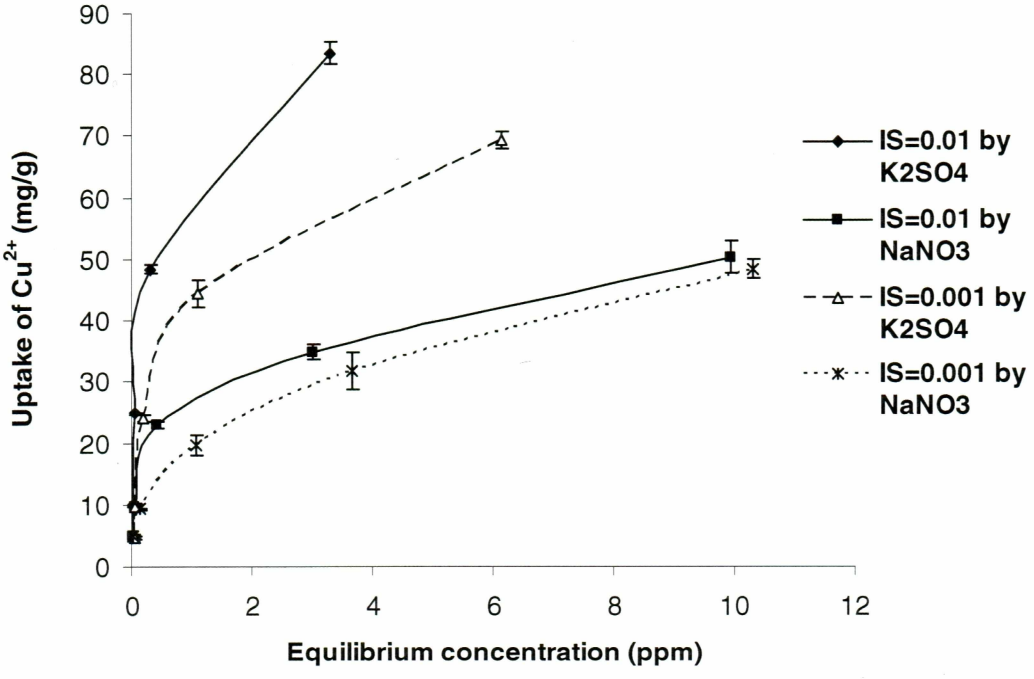

Fig. 5.10 Ionic strength effect on the adsorption of Cu^{2+} at pH 6 by DDA 80.7 chitosan

The reason for the elevated uptake at high ionic strength might be a more significant sorbent network swelling encouraged by high ionic strength. The polymer

network carries a fixed positive charge. With this fixed charge, the polymer itself can act as a Donnan phase. It was observed (Flory, 1969) that the concentration of mobile ions was always greater in the network than outside. Consequently, the osmotic pressure difference between inside and outside the network acted as the driving force to expand the network with water diffusing into the network to counteract the higher concentrations of mobile ions. The equation describing how swelling of an ionic network is affected by the ionic strength was developed by Flory (1969):

$$Q_m^{5/3} = [(S^{*1/2} \times i / 2V_u)^2 + (1/2 - \chi_1)/V_1]/(v_e / V_0) \qquad (5\text{-}4)$$

where Q_m is the maximum swelling ratio in change of volume; i is the number of electronic charges per polymer unit; V_u is the molecular volume of the repeating unit; i/V_u represents the concentration of fixed charge referred to the unswollen network; S* is the ionic strength; χ_1 is the parameter expressing the first neighbor interaction free energy, divided by KT, for solvent with polymer; V_1 is the molar volume of solvent; v_e is the effective number of chains in the network; V_0 is the volume of unswollen network.

According to the equation, it is obvious that an increase of ionic strength will increase the expansion of the network, which exposes more functional sites for metal binding. That explains why the uptake of Cu^{2+} was higher at higher ionic strength. Similar results were reported previously by Mitani (1995) who found that the removal efficiencies of Co^{2+} and Ni^{2+} by chitosan tended to increase with an increase ionic strength.

To understand why sulfate had a more pronounced effect on the adsorption of Cu^{2+} than nitrate, it must be noted that in the current case the surface was slightly

positively charged, which repelled the positively charged sorbate. Both sulfate and nitrate added into the solution weakened the repulsion force between the surface and the sorbate by increasing the concentration of counterions in the electrolyte double layer. However, since SO_4^{2-} reacted with the functional sites and neutralized the surface charge while NO_3^- did not, the uptake was increased more by adding SO_4^{2-} into the solution. The measurement of zeta potential of the sorbent surface (shown in Table 5.1) confirmed that the addition of sulfate significantly reduced the zeta potential while the addition of nitrate had much less effect.

Table 5.1 Surface zeta potential of chitosan particles with DDA=80.7 under different conditions

No.	Salt	IS (M)	Zeta potential (mV)
1	None	0	39.52 ± 0.66
2	$NaNO_3$	0.01	31.96 ± 0.34
3	K_2SO_4	0.01	16.01 ± 1.43

In fact, the influence of sulfate should be universal for all types of metal cations since it changes sorbent properties. An increase in uptake was also observed for adsorption of Cd^{2+} with sulfate in the solution. In Fig. 5.10, adding sulfate did not change the linear shape of the adsorption isotherm, but increased the slope of the line from 1.2 to 4.7.

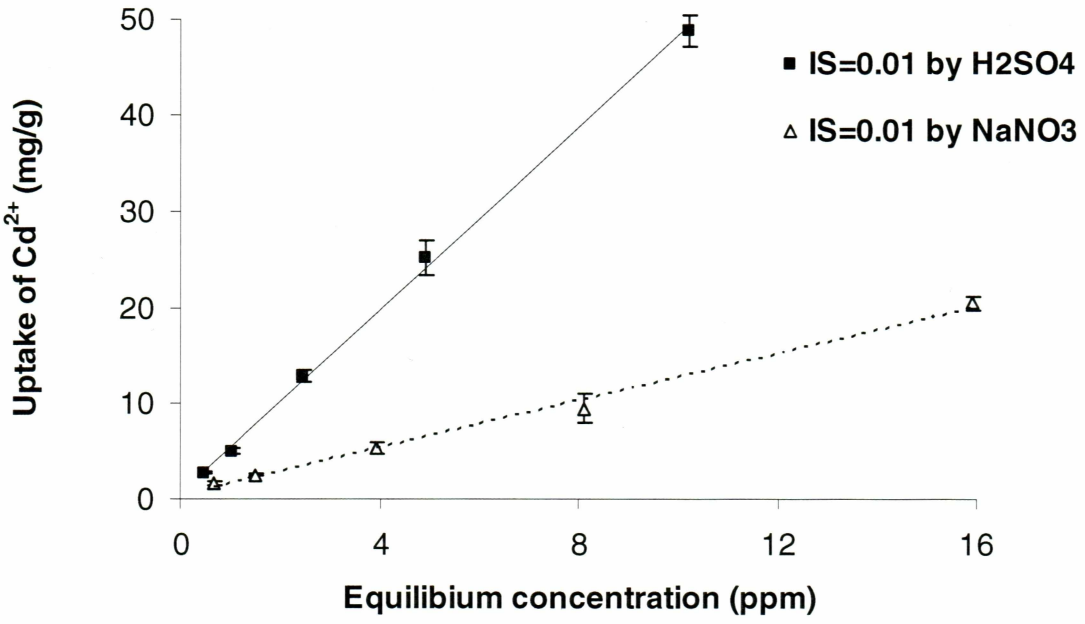

Fig. 5.11 Effect of different types of salts on the adsorption of Cd^{2+} by chitosan with DDA=80.7 at pH 7

Chapter 6

Conclusions and future work

A series of sorbents developed from crab shells demonstrate the capacity to adsorb heavy metals from solution with the removal efficiencies depending both on the type of metal and the characteristics of the sorbents. The research first provided an evaluation of the analytical approaches in characterizing the sorbents, and then compared the removal efficiency of both Cu^{2+} and Cd^{2+} by each sorbent. Other parameters such as pH and ionic strength of the solution were also studied. In this chapter the results and conclusions of this study are summarized, followed by recommendations for future work.

6.1 Conclusions

1) The FTIR calibrated by NMR serves as a reliable method for determining the DDA as long as the right baseline method is chosen and calibrated by the standard DDA.

2) Potentiometric titration is not a valid method for DDA measurement, especially for the samples within the medium DDA range, because the amount of titrable sites does not equal the total amount of amino groups.

3) A series of potential sorbents can be developed from waste crab shells. Among them, the raw crab shell does not show significant uptake of metals, and acid-washed crab shells adsorbed both Cu^{2+} and Cd^{2+}. The removal efficiency was lower than that of chitinous sorbents for adsorption of Cu^{2+}, but higher than that of chitinous polymers for Cd^{2+} adsorption. The results suggested that the protein co-existing with chitin adsorbed metals, and Cd^{2+} had higher affinity to protein than to chitin. The most important factor affecting the adsorption efficiency of chitinious sorbents is the degree of deacetylation

(DDA). The adsorption capacity increased with the increase of DDA for both Cu^{2+} and Cd^{2+}, which confirmed the idea that the amino groups had higher affinity to metals than acetyl-amide groups.

4) pH has a significant effect on the adsorption of metal ions on chitinous sorbents. The adsorption increases at higher pH. Since the surface of the sorbent is positively charged at low pH, tending to repel the positively charged metal ions, the metal ion needs to be more competitive than the proton to bind on the adsorption sites for pH values below the pK_a value. As the pH rose, the surface approached neutral charge, and more metal ions were adsorbed.

5) Conditioning chitosan with sulfuric acid stabilizes the sorbent and bonds excess protons in the network which causes low uptake if the adsorption is conducted under low pH, but if the pH of the solution is high and the protons in the network are allowed to release, the uptake by the conditioned chitosan is similar to that by the unconditioned chitosan.

6) The adsorption of both Cu^{2+} and Cd^{2+} increased at elevated ionic strength, which might be related to easier diffusion through the polymer. High ionic strength accelerated the expansion of the network, leading to higher accessibility of the functional sites. Added sulfate could reduce the repulsion of metal cations by the positive surface charge and greatly stimulated the adsorption of metal ions.

6.2 Future work

Results from this study indicated that the protein bonded with chitin in crab shells may also play an important role in adsorbing Cd^{2+} and Cu^{2+}. It is worthwhile to

investigate the adsorption of those metals by pure protein to verify whether the uptake by acid-washed crab shell is caused by protein or not.

Conditioning chitosan with H_2SO_4 stops the dissolution while conditioning with K_2SO_4 does not significantly reduce the extent of dissolution. The explanation made by the author is that since H^+ can attach to the amino groups while K^+ can not, H_2SO_4 crosslinks the polymer and K_2SO_4 does not. It will be interesting to do more experiments to test a general hypothesis: the ionic crosslink happens when opposite charges bind on the amino groups at the same time and attract each other.

Sulfate addition to the solution stimulated the metal ion adsorption to a larger extent than nitrate in this study. One possible reason could be that sulfate reacted with the functional groups on the sorbent and reduced the repulsion force between the surface and the metal ions. Other oxyanions such as molybdate, vanadate and phosphate, which are known to react with chitosan, could be tested for their effect on the adsorption to verify the idea that reducing the surface charge causes more adsorption.

Another topic worth of study would be how much crosslinking changes the chitosan structure and its swelling behavior. The extent of swelling can be tested by comparing the water content or by comparing the particle size of chitosan and sulfate conditioned chitosan at different pH.

References

US EPA, "Drinking Water Contaminants." Ground Water and Drinking Water. 28 November 2006. US Environmental Protection Agency <http://www.epa.gov/safewater/mcl.html>

Baxter A.; Dillon M.; Taylor K. D.; Roberts G. A. Improved method for I.R. determination of the degree of N-acetylation of chitosan. *International Journal of Biological Macromolecules* **1992**, 14, 166-169.

Berger, J.; Reist, M.; Mayer, J. M.; Felt, O.; Peppas, N. A.; Gurny, R. Structure and interactions in covalently and ionically crosslinked chitosan hydrogels for biomedical applications. *European Journal of Pharmaceutics and Biopharmaceutics* **2004**, 5, 19-34.

Berthold, A.; Cremer, K.; Kreuter. Influence of crosslinking on the acid stability and physicochemical properties of chitosan microspheres. *S.T.P. Pharmacy Sciences* **1996**, 6(5), 358-364.

Chen, R; Hua, H. Effect of N-Acetylation on the acidic solution stability and thermal and mechanical properties of membranes prepared from different chain flexibility chitosan. *Journal of Applied Polymer* Science **1996**, 61, 749-754.

Chu, K. H. Removal of copper from aqueous solution by chitosan in prawn shell: adsorption equilibrium and kinetics, *Journal of Hazardous Materials* **2002**, B90, 77-95.

Comyn, J. (Ed), *Polymer Permeability*, Elsevier applied publishers, **1985**.

Davis, T.; Volesky, B.; Mucci, A. A review of the biochemistry of heavy metal biosorption by brown algae, *Water Research* **2003**, 37, 4311-4330.

Ding, C.; Song, Q.; Ye, S. Adsorption mechanism and preparation of chitosan-Zn^{2+} complex. *Journal of East China University of Science and Technology* **2003**, 29, 315-316, 324.

Domszy, J.G. and Roberts, G.A.F. Evaluation of infrared spectroscopic techniques for analyzing chitosan, *Makromolekulare Chemie* **1985**, 186, 1671-1677.

Duarte, M.L., Ferreira, M.C., Marvao, M.R., Rocha, J. An optimized method to determine the degree of acetylation of chitin and chitosan by FTIR spectroscopy. *International Journal of Biological Macromolecules* **2002**. 31, 1-8.

Filar, L. J.; Wirick, M. G. Bulk and solution properties of chitosan. *MITSG 78-7, Proceeding of International Conference of Chitin/Chitosan, 1st,* **1977**, 169-181.

Flory, Paul J. *Principles of Polymer Chemistry,* Cornell University Press, **1969**.

Focher, B.; Beltrame, P. L.; Naggi, A.; Torri, G. Alkaline N-Deacetylation of chitosan enhanced by flash treatment. Reaction kinetics and structure modifications. *Carbohydrate Polymer.* **1990**, 12, 405-418.

Guibal, E.; Dambies, L.; Milot, C.; Roussy, J. Influence of polymer structural parameters and experimental conditions on metal anion sorption by chitosan, *Polymer International*, **1999**, 48, 671-680.

Guo, X.; Kikuchi, K.; Matahira, Y.; Sakai, K.; Ogawa, K., J. Water-soluble chitin of low degree of deacetylation. *Carbohydrate Chemistry* **2002**, 21 (1&2), 149-161.

Hirai, A; Odani, H.; Nakajima, A. Determination of degree of deacetylation of chitosan by proton NMR spectroscopy. *Polymer Bulletin* **1991**, 26, 87-94.

Jaworska, M; Sakurai, K; Gaudon, P; Guibal, E. Influence of chitosan characteristics on polymer properties. I: Crystallographic properties. *Polymer International* **2003**, 52(2), 198-205.

Jha, I. N.; Iyengar, L; Rao, A. Prabhakara V. S. Removal of cadmium using chitosan, *Journal of Environmental Engineering*, **1998**, 114, 962-74.

Khor, E. Chitin: fulfilling a biomaterials promise. **2001**, Elsevier, Oxford, UK.

Kim, C Y; Choi, H-M; Cho, H T. Effect of deacetylation on sorption of dyes and chromium on chitin, *Journal of Applied Polymer Science* **1997**, 63, 725-736.

Kim, D. S; Park, B. Y. Effect on the removal of Pb^{2+} from aqueous solution by crab shell, *Journal of Cheminal Technology and Biotechnology*. **2001**, 76, 1179-1184.

Kristbergsson K; Einarsson, J. M.; Martin, G.P. Recent developments in deacetylation of chitin and possible application food formulation, *Transaction of the Atlantic Fisheries Technology Conference* **2003**.

Kurita, K; Sannan, T; Iwakura, Y. Studies on chitin. VI. Binding of metal cations. *Journal of Applied Polymer Science* **1979,** 23, 511-515.

Kurita, K; Sannan, T; Iwakura, Y. Studies on chitin 4. Evidence for formation of block and random copolymers of N-acetyl-D-glucosamine and D-glucosamine by hetero- and homogeneous hydrolyses. *Makromolekulare Chemie* **1977**, 178, 3197-3202

Lasko, C. L.; Adams, K. H.; Debenedet, E. M.; West, P. A. A simple sulfuric acid pretreatment method to improve the adsorption of Cr(VI) by chitosan, *Journal of Applied Polymer Science* **2004**, 93, 2808-2814.

Lavertu, M.; Xia, Z.; Serreqi, A. N.; Berrada, M.; Rodrigues, A.; Wang, D.; Buschmann, M. D.; Gupta, A. A validated ^{1}H NMR method for the determination of the degree of deacetylation of chitosan. *Journal of Pharmaceutical and Biomedical. Analysis* **2003**, 32, 1149-1158.

Li, N; Bai, R. A novel amine-shielded surface crosslinking of chitosan hydrogel beads for enhanced metal adsorption performance, *Industrial & Engineering Chemistry Research* **2005**, 44, 6692-6700.

Mcafee, B.J.; Gould, W.D.; Nadeau, J.C.; Costa, A.C.A. Biosorption of metal ions using chitosan, chitin, and biomass of Rhizopus Oryzae. *Separation Science and Technology* **2001**, 36, 3207-3222.

Mao, S; Shuai, X; Unger, F; Simon, M; Bi, D; Kissel, T. The depolymerization of chitosan: effects on physicochemical and biological properties. *International Journal of Pharmaceutics* **2004**, 281, 45-54.

Mima, S; Miya, M; Iwamoto, R.; Yoshikawa, S., Highly Deacetylated Chitosan and Its Properties, *Journal of Applied Polymer Science*, **1983**, 28, 1909-1917.

Mitani, T.; Nakajima, C.; Sungkono, I. E.; Ishii, H. Effect of ionic strength on the adsorption of heavy metal by swollen chitosan beans, *Journal of Environmental Science and Health* **1995**, A30, 669-674.

Muzzarelli, R.A.A. *Chitin*, Pergamon Press: Oxford, **1977**

Muzzarelli, R.A.A; Rocchetti, R. Enchanced capacity of chitosan for transition-metal ions in silfate-sulfuric acid solutions, *Talanta* **1974**, 21, 1137-1143.

Niu H., Volesky, B. Biosorption mechanisms for anionic metal species with waste crab shells, *The European Journal of Mineral Processing Environmental Protection*, **2003**, 3, 75-87

Park, J. W.; Park, M. O.; Park, K. K. Mechanism of metal ion binding to chitosan in solution. Cooperative inter- and intramolecular chelations. *Bulletin of the Korean Chem. Soc.* **1984**, 5, 108-12.

Piron, E.; Domard, A. Interaction between chitosan and uranyl ions Part 1 Role of physicochemical parameters, *Int. J. Biol. Macromol* **1997,** 21, 327-335

Piron, E.; Domard, A. Interaction between chitosan and uranyl ions. Part 2. Mechanism of interaction, *Int. J. of Biol. Macromol* **1998**, 22, 33-40.

Rhazi, M; Desbrieres, J; Tolaimate A; Alagui A; Vottero P. Investigation of different natural sources of chitin: influence of the source and deacetylation process on the physicochemical characteristics of chitosan, *Polymer International* **2000**, 49, 337-344.

Sabnis, S. and Block, L.H., Improved infrared spectroscopic method for the analysis of degree of N-deacetylation of chitosan, *Polymer Bulletin (Berlin)* **1997**, 39, 67-71.

Sannan, T.; Kurita, K.; Iwakura, Y., Study on Chitin. 1. Solubility change by alkaline treatment and film casting, *Die Makromolekulare Chemie* **1975**, 176, 1191-1195.

Shigemasa, Y.; Matsuura, H.; Sashiwa, H., Saimoto, H. Evaluation of different absorbance ratios from infrared spectroscopy for analyzing the degree of deacetylation in chitin, *Int. J. Biol. Macromol.* **1996**, 18, 237-242.

Sorlier, P.; Denuziere, A.; Viton, C., Domard, A. Relation between the degree of acetylation and the electrostatic properties of chitin and chitosan, *Biomacromolecules* **2001**, 2, 765-772.

Stumm, W., *Chemistry of the Solid-Water Interface*, A Wiley-Interscience Publication, **1992.**

Suder, B J; Wightman, J. P. Interaction of heavy metals with chitin and chitosan. II. Cadmium and zinc. Editor(s): Ottewill, R. H.; Rochester, C. H.; Smith, A. L. Symposium on *Adsorption from Solution* **1983**, 235-244.

Suryanarayana, C.; Grant Norton, M. *X-Ray Diffraction A Practical Approach*, Plenum Press: New York, **1998**.

Volesky, B. (Ed.), *Biosorption of Heavy Metals*, CRC Press, Boca Raton, FL, **1990**.

Wang, Z.; Wang, S.; Huang, Y. Study of adsorption mechanism of chitosan for Cd^{2+} by x-ray photoelectron spectrometry, *Chinese Journal of Analysis Laboratory* **2001**, 20, 14-16.